Available online at www.sciencedirect.com
SCIENCE DIRECT®
ELSEVIER
International Journal of Pharmaceutics 314 (2006) 101–119
INTERNATIONAL JOURNAL OF PHARMACEUTICS
www.elsevier.com/locate/ijpharm

Review

Local controlled drug delivery to the brain: Mathematical modeling of the underlying mass transport mechanisms

J. Siepmann [a,b,*], F. Siepmann [b], A.T. Florence [c]

[a] *College of Pharmacy, Freie Universitaet Berlin, Kelchstr. 31, 12169 Berlin, Germany*
[b] *College of Pharmacy, University of Lille, 3 rue du Professeur Laguesse, 59006 Lille, France*
[c] *School of Pharmacy, University of London, 29/39 Brunswick Square, WC1N 1AX London, UK*

Received 11 May 2005; accepted 12 July 2005

Abstract

The mass transport mechanisms involved in the controlled delivery of drugs to living brain tissue are complex and yet not fully understood. Often the drug is embedded within a polymeric or lipidic matrix, which is directly administered into the brain tissue, that is, intracranially. Different types of systems, including microparticles and disc- or rod-shaped implants are used to control the release rate and, thus, to optimize the drug concentrations at the site of action in the brain over prolonged periods of time. Most of these dosage forms are biodegradable to avoid the need for the removal of empty remnants after drug exhaustion. Various physical and chemical processes are involved in the control of drug release from these systems, including water penetration, drug dissolution, degradation of the matrix and drug diffusion. Once the drug has been released from the delivery system, it has to be transported through the living brain tissue to the target site(s). Again, a variety of phenomena, including diffusion, drug metabolism and degradation, passive or active uptake into CNS tissue and convection can be of importance for the fate of the drug. An overview is given of the current knowledge of the nature of barriers to free access of drug to tumour sites within the brain and the state of the art of: (i) mathematical modeling approaches describing the physical transport processes and chemical reactions which can occur in different types of intracranially administered drug delivery systems, and of (ii) theories quantifying the mass transport phenomena occurring after drug release in the living tissue. Both, simplified as well as complex mathematical models are presented and their major advantages and shortcomings discussed. Interestingly, there is a significant lack of mechanistically realistic, comprehensive theories describing both parts in detail, namely, drug transport in the dosage form and in the living brain tissue. High quality experimental data on drug concentrations in the brain tissue are difficult to obtain, hence this is itself an issue in testing mathematical approaches. As a future perspective, the potential benefits and limitations of these mathematical theories aiming to facilitate the design of advanced intracranial drug delivery systems and to improve the efficiency of the respective pharmacotherapies are discussed.
© 2006 Elsevier B.V. All rights reserved.

Keywords: Controlled release; Brain; Mathematical modeling; Transport mechanisms; Diffusion

Contents

* Corresponding author. Tel.: +33 3 20964708; fax: +33 3 20964942.
E-mail address: juergen.siepmann@univ-lille2.fr (J. Siepmann).

0378-5173/$ – see front matter © 2006 Elsevier B.V. All rights reserved.
doi:10.1016/j.ijpharm.2005.07.027

1. Introduction

The treatment of diseases of the central nervous system (CNS) following systemic drug administration is challenging because of the existence of the blood–brain barrier (BBB) (Abott and Romero, 1996; Wang et al., 2002a). Generally, only low molecular weight, lipid-soluble molecules and a few peptides and nutrients can cross this barrier to any significant extent, either by passive diffusion or using specific transport mechanisms (Grieg, 1987). So, for most drugs it is not possible to achieve therapeutic levels within the brain tissue following intravenous or oral administration. In addition, highly potent drugs (e.g., anticancer drugs and neurotrophic factors) that may be necessary to be delivered to the CNS, often cause serious toxic side effects when administered systemically.

To overcome these restrictions, the drug can be administered directly into the brain tissue (Wang et al., 2002a). In such intracranial modalities, the BBB is breached by avoidance. However, this administration route carries considerable risk of CNS infections, and most drugs are rapidly cleared from brain tissue, exhibiting only short half-lives, this is a serious restriction. Therapeutic drug concentrations at the target site might only be achieved during very short time periods and the efficiency of the treatments would be very limited. Biodegradable drug delivery systems which are able to control the release rate of an incorporated drug in a pre-determined manner over periods of days to months offer an interesting possibility to overcome this restriction (Langer and Folkman, 1976; Langer and Wise, 1984; Leong et al., 1985; Chasin and Langer, 1990; Tamargo et al., 1991, 1993; Brem et al., 1993; Brem and Langer, 1996; Wang et al., 2002a). Ideally, one single intracranial administration would be sufficient to provide therapeutic drug levels at the site of action for prolonged periods of time.

To control the release rate of a drug, it can for example be embedded in a polymeric or lipidic matrix. Different mechanisms (e.g., diffusion, degradation and dissolution) will then be involved in the control of its release (Langer, 1980; Langer and Wise, 1984; Baker, 1987; Ron and Langer, 1992; Siepmann and Goepferich, 2001). Several types of intracranially administered controlled drug delivery systems (which are generally based on biodegradable polymers) have been proposed and tested in vitro as well as in vivo (Langer and Folkman, 1976; Langer and Wise, 1984; Chasin and Langer, 1990; Lee et al., 2005). These devices have the major advantage of: (i) avoiding difficulties of gaining access to the brain parenchyma across the BBB, (ii) avoiding the necessity of surgical removal after drug exhaustion and (iii) being able (in principle) to maintain desired drug levels at the target sites over prolonged periods of time. The question of what are optimum drug levels to achieve total cell eradication has, however, not always been ascertained.

Different CNS diseases can be treated with intracranially administered controlled drug delivery systems, principally brain tumors and neurodegenerative disorders such as Parkinson's and Huntington's diseases (Langer, 1991; Menei et al., 1994; Mittal et al., 1994; Benoit et al., 2000). The efficiency of various devices has been investigated in animal models (Yang et al., 1989; Grossman et al., 1992; Ewend et al., 1996; Sipos et al., 1997; Fung et al., 1998) and some systems have also been subjected to clinical trials (Brem et al., 1991, 1995a, 1995b; Valtonen et al., 1997; Menei et al., 1999, 2005). The first (and so far only) pharmaceutical product that is available on the market based on the principle of intracranial controlled drug delivery is Gliadel® (Brem et al., 1995b; Valtonen et al., 1997). It comprises a disc-shaped wafer, consisting of BCNU (1,3-bis(2-chloroethyl)-1-nitrosourea; carmustine) as the drug (loading: 3.85%) and poly[bis(*p*-carboxyphenoxy)] propane–sebacic acid (PCPP:SA) as the biodegradable polymer. Gliadel® was developed in the early to mid 1990's by the group of Henry Brem and obtained Food and Drug Administration (FDA) approval in 1996 for the treatment of recurrent glioblastoma multiforme. The basic principle of this treatment method for operable tumors is that the tumor is removed from the brain tissue and as large quantities of surrounding tissue cannot be removed concurrently because of the risk to affect vital brain functions. The probability is that individual viable tumor cells remain within the brain (infiltrated neighboring tissue). Many patients die due to local tumor recurrence in the vicinity of the primary tumor. To reduce this risk one or more disc-shaped, BCNU-loaded wafers are placed into the resection cavity of the tumor (during the same operation) (Fig. 1). The anticancer drug is then released in a time-controlled manner into the resection cavity and penetrates into the surrounding tissue. The questions are two-fold: once released, how far can the drug penetrate, in other words what is its zone of activity and what is the optimal level of drug over what period of time to achieve tumor cell death?

A *multiparticulate* drug delivery system for the same type of treatment has been proposed by the groups of Benoit and Menei (Menei et al., 1999, 2005; Roullin et al., 2002): 5-fluorouracil (5-FU)-loaded poly(lactic-co-glycolic acid) (PLGA)-based microparticles. These microparticles have the advantage that they can be administered by stereotaxic means using standard syringes. Thus, both operable and inoperable tumors can be treated. In the first case, the tumor is removed from the brain tissue and the microparticle suspension is injected at multiple locations into the wall of the resection cavity (Fig. 2). This offers the advantage of reaching deeper tissue regions, thus overcoming potential problems of restricted drug penetration

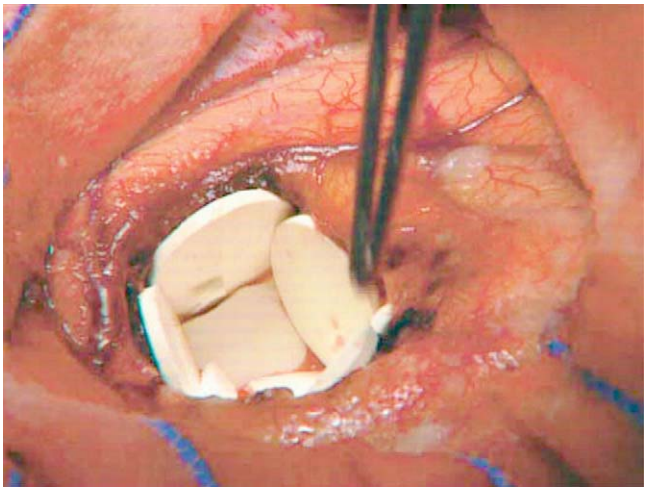

Fig. 1. Principle of the treatment of recurrent glioblastoma multiforme with Gliadel®. Upon tumor resection, up to eight anticancer drug-loaded polymeric wafers are placed into the resection cavity. The drug is then released in a time-controlled manner from the wafers into the cavity and surrounding tissue (reprinted with permission from Moses et al., 2003).

into the brain tissue. The microparticles release the drug in a time-controlled manner over several weeks. A phase IIb clinical trial with this treatment method has recently shown promising results (Menei et al., 2005). Furthermore, the microparticles can be injected into inoperable tumors. A phase I clinical trial recently demonstrated the feasibility of this treatment method (Menei et al., 2004).

Direct injection of formulations into tumors is not the panacea that it might appear because drug once released from microparticles can diffuse or leak through needle tracks. Direct injection of adenoviral vector into tumor cells causes viral escape. The use of the gel forming poloxamer 407 reduced viral escape by 100-fold as it blocked leakage through the needle track. However, microparticles should have an advantage over intratumorally injected drug solutions in this regard, although direct injection of adenoviral vectors in tumors allows viral escape, a problem reduced by a 100-fold by the administration of the viruses in a viscous gel-forming poloxamer. Major efforts have also been made to develop local controlled drug delivery systems to improve the treatment of neurodegenerative diseases, such as Alzheimer's and Parkinson's diseases (Saltzman et al., 1999). The idea is to deliver highly potent drugs (e.g., neurotrophic

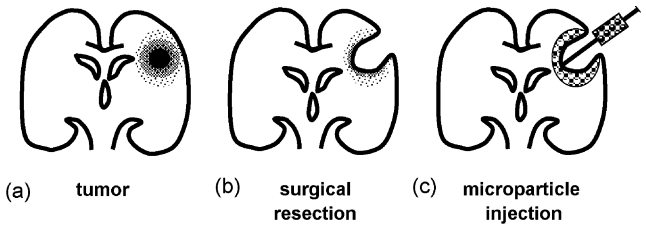

Fig. 2. Principle of the treatment of operable brain tumors with 5-fluouracil-loaded, PLGA-based microparticles. Schematic cross sections through a human brain. (a) The tumor is illustrated as a black circle; the surrounding tissue is infiltrated by single tumor cells. (b) The tumor has been removed surgically. (c) To minimize the risk of local tumor recurrence, drug-loaded microparticles are injected into the wall of the resection cavity at multiple locations.

factors) to the affected brain regions to stimulate the growth or retard the degradation of the respective CNS cell types. The drugs needed in these indications tend to be peptides as some have lower diffusion capacity in brain time and offer a greater challenge.

The design of advanced drug delivery system for the treatment of brain diseases is thus difficult because many factors are involved in the control of drug release out of the pharmaceutical dosage forms and of the subsequent drug transport through the living brain tissue to the site or sites of action (Haller and Saltzman, 1998a; Nicholson, 2001; Siepmann and Goepferich, 2001). For example, the physico-chemical properties of the drug and matrix former, the geometry and size of the device affect the resulting drug release kinetics and the anatomic characteristics of the healthy or pathologic brain tissue strongly influence subsequent distribution of action within the CNS. Hence, it is highly desirable to be able to identify and quantitatively describe the involved transport mechanisms (e.g., imbibition of biological fluid into the devices, drug diffusion, convective mass transfer processes). This can be achieved using as a basis appropriate experimental results and adequate mathematical theories. Obviously, the type of drug and release rate controlling polymer as well as the target site(s) and type/state of disease can fundamentally affect the relative importance of the involved phenomena. Thus, there is no overall mathematical model which will be valid for all types of drug delivery systems and diseases.

For each particular treatment method different experimental techniques should be used to understand better the phenomena which are involved in the control of drug release from the drug delivery system and the subsequent transport to the site(s) of action. Based on the different experimental results (where precision and accuracy have to be affirmed), adequate mathematical theories can be identified or developed to quantitatively describe the observed transport kinetics. These calculations allow the determination of system and disease specific parameters which can be used to identify the dominating chemical reactions and physical mass transfer processes (Siepmann and Goepferich, 2001; Siepmann and Peppas, 2001). Ideally, an adequate mathematical theory then permits the prediction of the effects of the most important formulation and processing parameters (for example, drug loading, shape and size of the device) on the resulting drug concentration–time profiles at the site(s) of action in the human brain in a quantitative way. Thus, the mathematical modeling also has an interesting practical application: it can help to both facilitate the optimization of the advanced drug delivery systems and improve the therapeutic efficiency of the treatments.

In the following, an overview is given on the current state of the art of mathematical modeling approaches describing: (i) drug transport within the pharmaceutical dosage forms and (ii) within the living brain tissue. Both simplified as well as complex theories are presented and their major advantages and shortcomings pointed out. Due to the significant number of variables, no effort is made in this review to present a uniform system of notation. Generally, the original nomenclature of the respective authors is followed (with sometimes slight modification to avoid misunderstandings). Interestingly, there is still a significant lack

of comprehensive mathematical models quantifying both drug transport within the dosage forms and drug transport within the brain tissue in a mechanistically realistic way. Without doubt experiment and theory agree that transport in the brain of all but the smallest drug molecules is hindered by a multiplicity of factors. The use, therefore, of biologically interesting endogenous molecules which are not only larger but also often labile presents enormous challenges to the development of new delivery devices and successful therapy. It is unlikely that new drugs alone will solve the problem of the therapeutic challenges we face with these CNS pathologies.

2. Drug transport within the pharmaceutical dosage forms

2.1. Overall mass transport mechanisms

Various pharmaceutical dosage forms can be used for local intracranial drug delivery. Generally, the drug is embedded within a polymeric or lipidic matrix which hinders its instantaneous dissolution or release. Biodegradable systems have the major advantage that they avoid the need for removal of remnants on drug depletion. Very different types of matrix formers and device geometries can be used. Practical examples include polyanhydride-based flat cylinders, PLGA-based spherical microparticles and lipidic rod-shaped implants.

Depending on the composition, dimension and sometimes even the preparation method of the system, different physical and chemical phenomena may be involved in the control of the resulting drug release kinetics, including:

- water penetration into the system
- drug dissolution
- dissolution/degradation of the matrix former
- precipitation and re-dissolution of degradation products
- structural changes within the system occurring during drug release, such as the creation/closure of water-filled pores
- changes in the microenvironmental pH (e.g., creation of acidic microclimates in PLGA-based delivery systems and subsequent autocatalysis of the polyester)
- diffusion of drug and/or degradation products of the matrix material out of the device with constant or time-dependent diffusion coefficients
- osmotic effects
- convection processes, and
- adsorption/desorption phenomena

In contrast to oral-controlled drug delivery systems, swelling of the matrix former is best avoided because of the limited space in the brain tissue. Intracranially administered devices which swell significantly can lead to serious side effects.

Generally, it is not reasonable to take all these phenomena into account, because this would lead to very complex mathematical models which are not suitable for routine use and require significant calculation times. Thus, one of the critical points when developing new or selecting adequate existing mathematical theories is to identify which are the *dominating* physical and chemical processes involved in the control of drug release from the specific system of interest. Only these phenomena should be considered in the mathematical theory. For example, if several processes occur sequentially and one of them is by far slower than all others, this step controls the overall rate of the whole sequence.

In certain systems, the physical and chemical processes can affect each other in a complex manner. For example, PLGA-based devices can show autocatalytic effects depending on their dimensions. Water penetration into PLGA-based microparticles and implants is known to be much faster than the subsequent ester bond cleavage (von Burkersroda et al., 2002). Thus, the entire drug delivery system is rapidly wetted and polymer degradation occurs throughout the device, generating shorter chain acids and alcohols. Due to concentration gradients the latter diffuse out of the dosage form. In addition, bases from the surrounding liquid environment diffuse down concentration gradients *into* the drug delivery system, neutralizing the generated acids. However, diffusional processes are generally slow and the rate at which the acids are produced within the dosage forms can be higher than the rate at which they are neutralized. Consequently, the microenvironmental pH within the system can drop significantly (Brunner et al., 1999; Li and Schwendeman, 2005). As ester bond cleavage is catalyzed by protons, this leads to accelerated polymer degradation and drug release (Siepmann et al., 2005). Device characteristics, such as porosity and size, can significantly affect the diffusion rates of the involved acids and bases and, thus, determine the underlying drug release mechanisms. Consequently, drug delivery systems of identical composition, which have been prepared using different techniques (resulting in different system properties, such as porosity) can exhibit very different drug release patterns due to altered drug release mechanisms.

2.2. Experimental measurement techniques

To be able to adequately model the mass transport mechanisms within a specific controlled drug delivery system, it is decisive to provide comprehensive experimental results on which to base the mathematical analysis. The physical and chemical characteristics of the system including its inner and outer structure, drug distribution, state of the drug and matrix former (e.g., amorphous, crystalline, molecularly dispersed should be known as well as potential changes in these properties occurring upon exposure to the release media (e.g., increase in porosity, decrease in polymer molecular weight of the matrix former, increase in mobility of the incorporated drug)). Various techniques can be used to provide these experimental results. In the following, only the most important ones are briefly discussed.

Obviously, the measurement of the resulting drug release kinetics is of fundamental importance. Different types of experimental in vitro apparatus and conditions have been proposed (Woo et al., 2001; Aubert-Pouessel et al., 2004). These include drug release into well agitated fluids in closed systems (e.g., using Pharmacopoeial paddle apparatus), into flowing liquids (e.g., using Pharmacopoeial flow-through cells) or into non-

agitated fluids or gels. Ideally, the conditions for drug release in vivo, in the living brain tissue, should be simulated. Crucial aspects to be addressed include the type of the release medium (e.g., with respect to pH, osmotic pressure, presence/absence of enzymes) as well as the degree of agitation and temperature (Faisant et al., 2006). Great care should be taken if physiologically unrealistic conditions are chosen. Sometimes the latter can be advantageous, rapidly allowing information on the quality of a batch ("stress" or "short term" tests for production), but the underlying drug release mechanisms might be very different from those obtaining under physiological conditions. Yet, no standard experimental apparatus has been established as a reference and it is often difficult to compare the results from different research groups. In the future it would be very helpful to define such a "standard" release experiment, ideally reflecting the conditions in vivo, to allow the establishment of meaningful in vitro–in vivo correlations.

If microparticles are studied, the determination of their average size and size distribution is of major importance, using a Coulter Counter or photon correlation spectroscopy (PCS) (Gref et al., 2001; Hedberg et al., 2004). Observation of changes in the microparticle size during drug release, such as disintegration into smaller fragments can be of outmost importance for a better understanding of the underlying drug release mechanisms (Siepmann et al., 2002).

In the case of biodegradable polymers as matrix formers, the extent of decrease in the average polymer molecular weight with time is very important information. The chain lengths of the polymer molecules determine their degree of entanglement and, thus, their mobility within the matrix. Polymer chain solubility is decisive for the velocity at which the drug can move within the polymeric network and, hence, for the resulting release kinetics. The average polymer molecular weight can be measured by gel permeation chromatography (Bittner et al., 1999; Kostanski et al., 2000).

Furthermore, the knowledge of the glass transition temperature (T_g) of the polymer is of major importance when studying underlying drug release mechanisms. If the matrix former is in the glassy state, the mobility of the macromolecules is much more restricted than in the rubbery state. This can have dramatic consequences on the diffusivity of the drug through the polymeric network, and release kinetics can significantly change when the polymer undergoes a glassy-to-rubbery phase transition. Differential scanning calorimetry (DSC) is used to determine the glass transition temperature of a system (Kranz et al., 2000; Jackson et al., 2004). In addition, DSC measurements can provide very valuable information on the state of the drug (e.g., crystalline or amorphous) and lipidic matrix formers. Various lipids used for controlled drug delivery systems show polymorphism. The modification of the matrix former can change during drug release (or during storage). These changes can significantly affect the resulting drug release mechanisms. Thus, this type of information is of major importance for the adequate modeling of the mass transport processes. To determine the crystallinity (and type of modification) of the drug and matrix former ideally both DSC and X-ray diffraction (Yilmaz et al., 2004) should be applied.

Microscopic techniques, including optical microscopy, scanning electron microscopy, atom force microscopy, can assist in understanding the underlying drug release mechanisms (Leo et al., 1998; Wang et al., 2002b). For example, the creation or closure of pores can be monitored and changes in the size and shape of the delivery systems followed. However, care has to be taken to avoid creation of artifacts. Some of the techniques require special sample treatment such as drying steps prior to the measurements. Drying can significantly alter the structure of the drug delivery systems (e.g., highly porous devices can collapse) and lead to erroneous conclusions.

In addition, electron paramagnetic resonance spectroscopy (EPR spectroscopy) and nuclear magnetic resonance (NMR) imaging techniques provide valuable information for the elucidation of the underlying drug release mechanisms. Interesting examples were reported by Maeder and co-workers (Maeder et al., 1997; Maeder, 2005; Richardson et al., 2005; Lurie and Maeder, 2005) on polyanhydride- and PLGA-based drug delivery systems. These techniques have also the decisive advantage to be applicable in vitro as well as in vivo.

2.3. Empirical and semi-empirical mathematical models

Empirical mathematical models are purely descriptive and cannot be used to gain insight into the mass transport mechanisms governing drug release from a particular dosage form. However, they can sometimes be helpful to provide a quantitative description of the observed drug release kinetics. Semi-empirical models are partially physicochemically realistic, but care has to be taken when drawing conclusions on the occurring physical and chemical phenomena.

A frequently used, semi-empirical model, that is very simple to apply, is the so-called power law:

$$\frac{M_t}{M_\infty} = kt^n \tag{1}$$

Here, M_t and M_∞ are the absolute cumulative amounts of drug released at time t and infinite time, respectively; k is a constant incorporating structural and geometric characteristics of the system, and n is the so-called "release exponent".

Peppas and co-worker (Peppas, 1985; Peppas and Korsmeyer, 1986) were the first to give an introduction into the use and limitations of the power law in the field of controlled drug delivery. In certain cases the exponent n can be indicative of the underlying drug release mechanism. For example, if (i) the drug delivery system has the geometry of a thin film that does not change its shape or size during the experiment (e.g., does not swell or dissolve) and (ii) the drug is homogeneously and molecularly dispersed throughout the system at $t = 0$ (before exposure to the release medium) (monolithic solution) and (iii) perfect sink conditions are maintained throughout the experiment, an exponent of $n = 0.5$ indicates purely diffusion-controlled drug release. It can be shown that a square root of time relationship between the cumulative amount of drug released and time is a good (early time) approximation for the exact solution of Fick's second law of diffusion under these conditions (valid for the first 60% of drug release) (Baker and Lonsdale, 1974). For other geometries,

the n values indicating purely diffusion-controlled drug release under these conditions are different, e.g. $n = 0.45$ for cylinders and $n = 0.43$ for spheres (Ritger and Peppas, 1987). Unfortunately, this fact is not always taken into account and sometimes certain assumptions (e.g., the fact that the matrix former must not dissolve to a significant extent during drug release) are violated.

Hopfenberg in 1976 proposed an interesting semi-empirical mathematical model to quantify drug release from an erodible pharmaceutical dosage form. The theory is based on the assumption that the release rate is proportional to the surface area of the device which is exposed to the release medium and which decreases with time. Importantly, all mass transfer processes involved in the control of drug release are assumed to add up to a single zero-order process. The latter can be characterized by a rate constant (k_0) which is confined to the surface area of the system. This zero-order process can correspond to one single physical or chemical phenomenon, but it can also result from the superposition of several processes, for example dissolution, swelling and polymer degradation. To simplify the analysis, edge and end effects are ignored. Hopfenberg derived the following equation, valid for different geometries:

$$\frac{M_t}{M_\infty} = 1 - \left(1 - \frac{k_0 t}{c_0 a}\right)^n \tag{2}$$

Here, M_t and M_∞ represent the cumulative amounts of drug released at time t and at infinite time, respectively; c_0 denotes the uniform initial drug concentration within the system; and a is the radius of a cylinder or sphere or the half-thickness of a slab. The exponent n is the so-called "shape factor", being equal to 3 for spheres, 2 for cylinders and 1 for thin films. The Hopfenberg model can, for example, be applied to surface eroding drug delivery systems with a zero-order surface detachment of the drug as the rate limiting release step.

2.4. Comprehensive mechanistic theories

Different mathematical theories have been reported for bioerodible controlled drug delivery systems, such as PLGA-based microparticles and thin films. For example, Charlier et al. (2000) presented an interesting model for bulk eroding polymer films. Importantly, polymer degradation and drug diffusion are considered simultaneously. Similar to the square root of time Higuchi model (Higuchi, 1961), a pseudo-steady state approach was used, which is valid for initial drug loadings well above the solubility of the drug within the system. The increase in drug mobility (diffusion coefficient, D) with time t (due to the decrease in the average polymer molecular weight) is considered to follow first-order kinetics:

$$D = D_0 \exp(kt) \tag{3}$$

where D_0 is the diffusion coefficient of the drug at $t = 0$ (prior to polymer degradation); and k the degradation rate constant. Based on these assumptions, the following equation for the cumulative absolute amount of drug released, Q, has been derived:

$$Q = S\sqrt{\frac{2c_0 c_s D_0[\exp(kt) - 1]}{k}} \tag{4}$$

where S is the surface area of the film exposed to the release medium; and c_0 and c_s are, respectively, the initial drug concentration and the solubility of the drug in the system. Good agreement between theoretical calculations and experimentally determined release kinetics of mifepristone from PLGA-based films was obtained (Charlier et al., 2000).

Recently, Raman et al. (2005) proposed an interesting mathematical model quantifying drug release from spherical PLGA-based microparticles. The theory considers drug diffusion, polymer degradation and potentially non-homogeneous drug distribution within the system at $t = 0$. The basic equation is Fick's second law of diffusion for spherical geometry:

$$\frac{\partial c}{\partial t} = \frac{1}{r^2}\frac{\partial}{\partial r}\left(r^2 D(M_w)\frac{\partial c}{\partial r}\right) \tag{5}$$

where c is the concentration of the drug, t is time, r the radial coordinate and $D(M_w)$ denotes the polymer molecular weight-dependent drug diffusivity.

For piroxicam-loaded, PLGA-based microparticles, the following empirical dependence of the diffusion coefficient D on the average polymer molecular weight (M_w) was found:

$$\ln D = -0.347(\ln M_w)^3 + 10.394(\ln M_w)^2 - 104.950(\ln M_w) + 316.950 \tag{6}$$

Furthermore, the following initial and boundary conditions were considered:

$$c(r)|_{t=0} = f(r) \tag{7}$$

$$\left.\frac{\partial c}{\partial r}\right|_{r=0} = 0 \tag{8}$$

$$c|_{r=R} = 0 \tag{9}$$

where R denotes the radius of the microspheres. The initial drug distribution within the systems ($f(r)$) was obtained from confocal micrographs.

The model was solved numerically and successfully fitted to experimentally determined piroxicam release data from PLGA-based microparticles exhibiting a very narrow particle size distribution (Berkland et al., 2001, 2003). Fig. 3 shows examples for these fittings for microparticles prepared with different PLGA types (the inherent viscosities in hexaflouroisopropanol as measures of the average polymer molecular weight) are indicated. Importantly, the entire drug release period is adequately described in all cases.

Monte Carlo simulations have shown to be very useful to model the random degradation of a polymeric matrix former. Zygourakis and co-worker (Zygourakis, 1989, 1990; Zygourakis and Markenscoff, 1996) was the first to use this type of approach to quantify drug release from surface eroding biodegradable delivery systems. Goepferich developed very comprehensive mathematical theories, combining Monte Carlo simulations (quantifying polymer degradation) with Fick's second law (describing drug diffusion) (Goepferich, 1996a, 1996b, 1997a, 1997b, 1997c; Goepferich and Langer, 1995a, 1995b; Goepferich et al., 1995). Importantly, these theories are applicable to both surface and bulk eroding polymeric systems

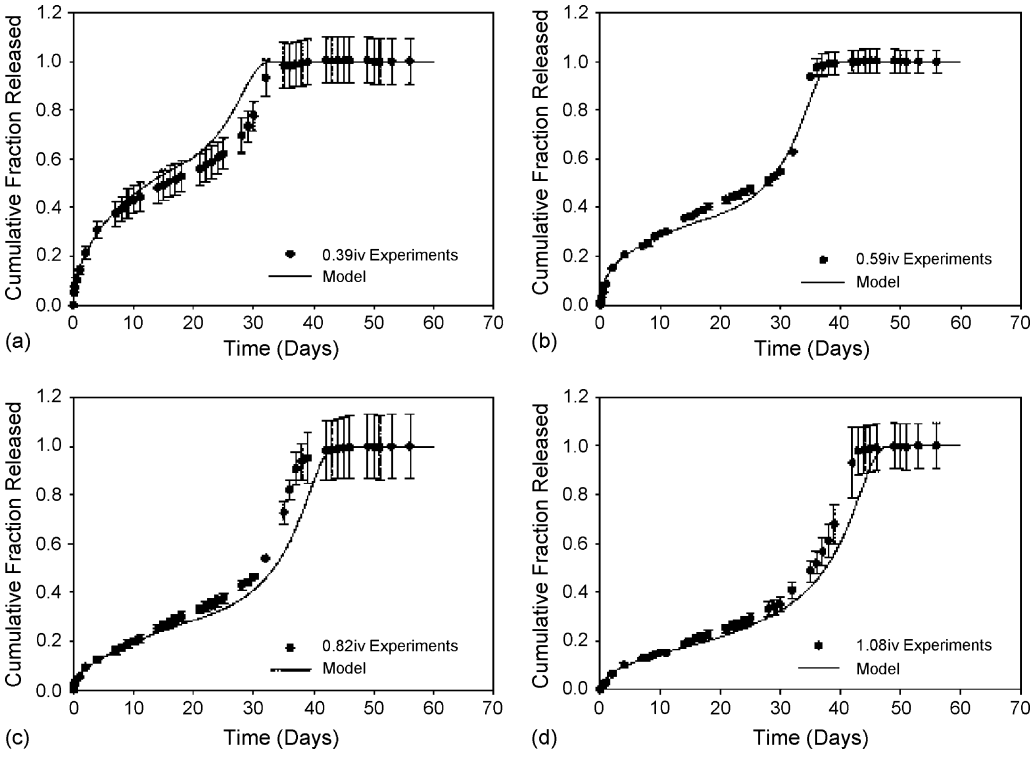

Fig. 3. Experiment (symbols) and theory (curves): fitting of the Raman model to experimentally determined piroxicam release from PLGA-based microparticles, differing in the average polymer molecular weight, designated by intrinsic viscosities as shown: (a) 0.39, (b) 0.59, (c) 0.82 and (d) 1.08 (reprinted with permission from Raman et al., 2005).

(Goepferich, 1997d). Furthermore, they have been extended to describe the erosion of three dimensional rotationally symmetric matrices (Goepferich and Langer, 1993), to describe the erosion of composite matrices made of bulk and surface eroding polymers (e.g., poly(D,L-lactic acid) and poly(CPP-SA)) (Goepferich, 1997a), and to quantify drug release from such composite devices (Goepferich, 1997b).

Siepmann et al. (2002) proposed a mathematical theory considering polymer degradation (based on Monte Carlo simulations), drug diffusion (based on Fick's second law) and potentially limited drug solubilities within the system. It is well known that water penetration into PLGA-based microparticles is more rapid than the subsequent hydrolytic degradation of the macromolecules (bulk erosion). However, due to the complexity of the systems, it is not possible to predict the exact time point at which a particular ester bond, located at a specific position within the macromolecular network, is cleaved. Fig. 4a shows a schematic presentation of such a spherical microparticle for mathematical analysis. To minimize computation time, it is assumed that the microparticle is rotationally symmetric to the angle θ. Thus, a two-dimensional grid (Fig. 4b) can be defined, which upon rotation around the z-axis describes the three-dimensional structure of the sphere. Considering symmetry planes in the planes with z and $r = 0$, the mathematical analysis can be further reduced to only one quarter of the two-dimensional circle (Fig. 5a). Each pixel represents either non-degraded polymer or drug (before the system is exposed to the release medium). Knowing the initial drug loading of the microparticles and the initial drug distribution within the systems, direct Monte Carlo techniques can be used to define which pixel represents non-degraded polymer and which pixel represents drug. Fig. 5a shows an example for a homogeneous initial drug distribution.

Importantly, all pixels are defined in such a way that they have the same height, but different widths. The coordinates are chosen to assure that the volumes of the cylindrical rings, which are described by the rectangular pixels upon rotation around the z-axis, are all equal. This results in about equal numbers of cleavable ester bonds within each ring. Thus, the probability with which the polymer pixels erode within a certain time period after contact with water can be assumed to be very similar (being essentially a function of the number of cleavable polymer bonds).

As polymer degradation is a random process, not all pixels degrade exactly at the same time point. Each pixel is characterized by an individual, randomly distributed "lifetime", t_{lifetime}, which can be calculated as follows as a function of the random variable ε (integer between 0 and 99):

$$t_{\text{lifetime}} = t_{\text{average}} + \frac{(-1)^{\varepsilon}}{\lambda} \ln\left(1 - \frac{\varepsilon}{100}\right) \tag{10}$$

where t_{average} is the average "lifetime" of the pixels, and λ is a constant (being characteristic for the type and physical state of the polymer). As soon as a pixel comes into contact with water, its "lifetime" starts to decrease. After the latter has expired, the pixel is assumed to erode instantaneously and to be converted into a water-filled pore.

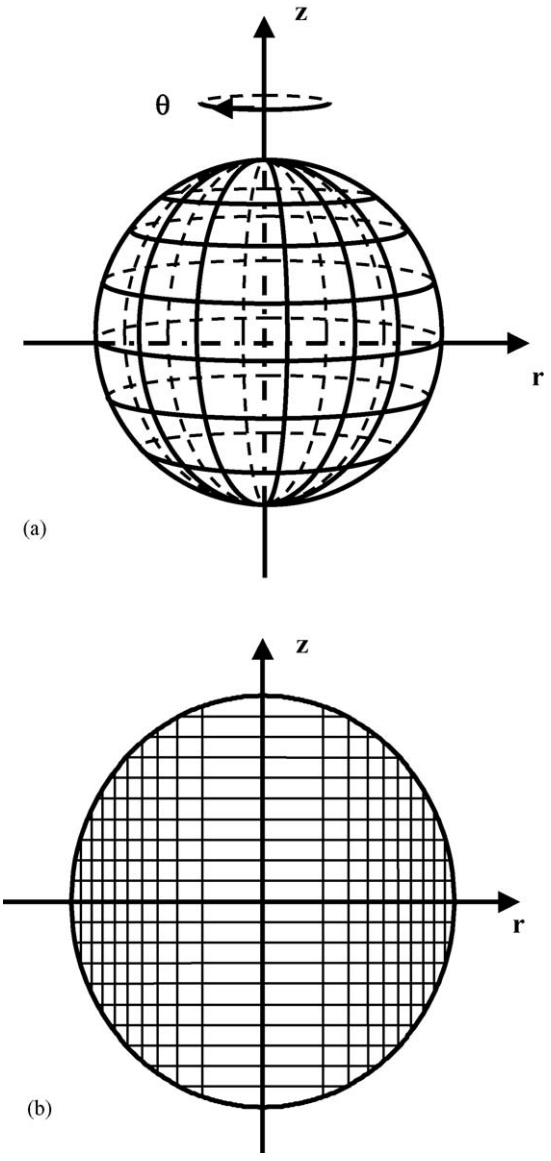

Fig. 4. Schematic presentation of a single bioerodible microparticle for mathematical analysis: (a) three-dimensional geometry; (b) two-dimensional cross section with two-dimensional pixel grid used for numerical analysis (reprinted with kind permission of Springer Science and Business Media from Siepmann et al., 2002).

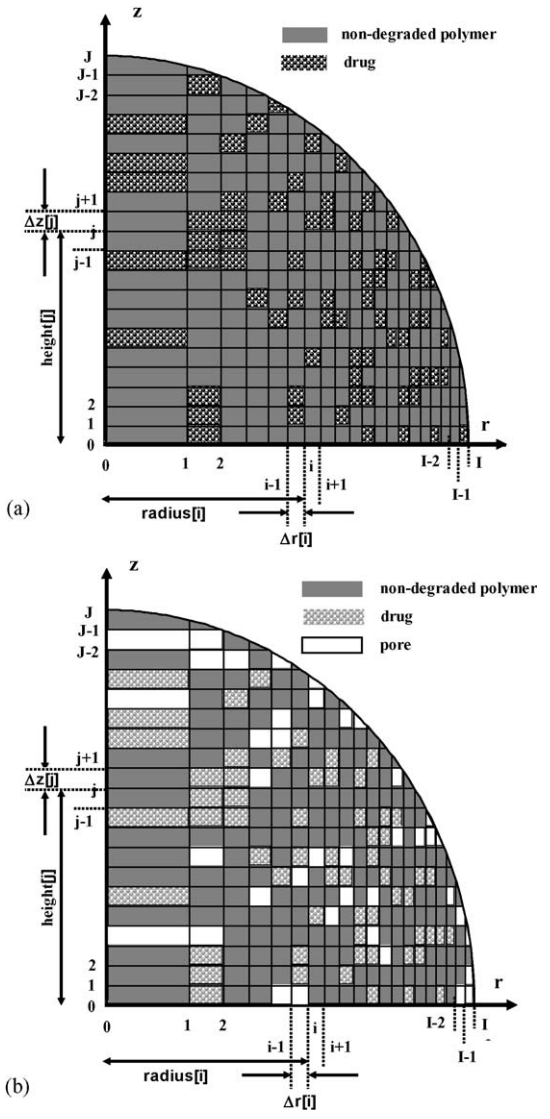

Fig. 5. Principle of the Monte Carlo-based approach to simulate polymer degradation and diffusional drug release; schematic structure of the system: (a) at time $t = 0$ (before exposure to the release medium); and (b) during drug release. Gray, dotted and white pixels represent non-degraded polymer, drug and pores, respectively (reprinted with permission of Springer Science and Business Media from Siepmann et al., 2002).

Once the initial condition (Fig. 5a) and the specific "life times" of all polymer pixels are defined, it is possible to determine the status of each pixel (representing drug, non-degraded polymer or a water-filled pore) at any time point. Fig. 5b shows an example for the composition and structure of a microparticle at a specific time point during drug release. This structural information is very important because it allows calculation of the porosity of the microparticles at any time point in both radial and axial directions, $\varepsilon(z, t)$ and $\varepsilon(r, t)$:

$$\varepsilon(r, t) = 1 - \frac{1}{n_z} \sum_{j=1}^{j=n_z} s(i(r), j, t) \tag{11}$$

$$\varepsilon(z, t) = 1 - \frac{1}{n_r} \sum_{i=1}^{i=n_r} s(i, j(z), t) \tag{12}$$

using the following "status function" s of the pixel $x_{i,j}$ at time t:

$$s(i, j, t) = 1, \quad \text{for non} - \text{eroded polymer} \tag{13}$$

$$s(i, j, t) = 0, \quad \text{for pores} \tag{14}$$

Here, n_z and n_r represent the number of pixels in the axial and radial direction at r and z, respectively.

Using Eqs. (11) and (12), the time- and direction-dependent porosities within the microparticles can be calculated at any grid point. These are essential pieces of information for the accurate calculation of the time-, position- and direction-dependent dif-

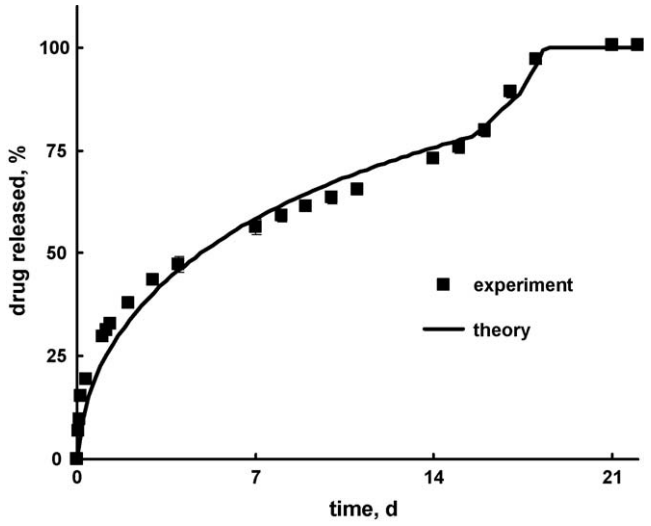

Fig. 6. Experiment (symbols) and theory (curve): fitting of a Monte Carlo-based mathematical model to experimentally determined 5-fluorouracil release from PLGA-based microparticles (reprinted with permission of Springer Science and Business Media from Siepmann et al., 2002).

fusivities:

$$D(r,t) = D_{\text{crit}}\varepsilon(r,t) \tag{15}$$

$$D(z,t) = D_{\text{crit}}\varepsilon(z,t) \tag{16}$$

where D_{crit} represents a critical diffusion coefficient, being characteristic for a specific drug–polymer combination.

These equations can be combined with Fick's second law of diffusion. The resulting set of partial differential equations must be solved numerically due to the non-constant diffusion coefficients. Using this model, good agreement between the experimentally determined and theoretically calculated release of 5-fluorouracil from PLGA-based microparticles (which are used for the treatment of brain tumors) was obtained (Fig. 6).

Surprisingly, there is still a significant lack of mathematical models taking autocatalytic effects (Cordes and Bull, 1974) within the drug delivery system into account, despite the considerable practical importance of this phenomenon (Klose et al., 2006). An interesting theory for poly(orthoester)-based thin films has been proposed (Thombre and Himmelstein, 1985; Joshi and Himmelstein, 1991; Thombre, 1992), while Siepmann et al. (2005) presented a model for PLGA-based microparticles. The latter is based on an analytical solution of Fick's second law of diffusion for spherical geometry:

$$\frac{M_\infty - M_t}{M_\infty} = \sum_{n=1}^{\infty} \frac{6S^2}{\beta_n^2(\beta_n^2 + S^2 - S)} \exp\left(-\frac{\beta_n^2}{R^2} Dt\right) \tag{17}$$

where M_∞ and M_t denote the absolute cumulative amounts of drug released at infinite time and time t, respectively; R is the radius of the sphere; D represents the diffusion coefficient of the drug and the β_ns are the roots of:

$$\beta_n \cot \beta_n = 1 - S \tag{18}$$

with the dimensionless number:

$$S = \frac{kR}{D} \tag{19}$$

The values of β_n are given in tables for various values of S (Crank, 1975; Vergnaud, 1993).

Fitting this set of Eqs. (17)–(19) to experimentally determined lidocaine release profiles from different-sized PLGA-based microparticles, facilitates calculation of the apparent diffusion coefficients of the drug within the polymeric systems. The mobility of lidocaine significantly increased with increasing system dimension, indicating that autocatalysis plays a major role: increasing diffusion pathway lengths lead to decreased neutralization rates of the generated acids and, thus, to decreasing microenvironmental pH values. The acidic microclimate accelerates polymer degradation and, consequently, increases the mobility of the drug molecules. This fact must adequately be taken into account when designing and optimizing this type of biodegradable microparticles. Interestingly, a quantitative relationship between the drug diffusivity, D, and the radius of the device, R, could be established:

$$D\,(\text{cm}^2/\text{s}) = 1.1 \times 10^{-15} R\,(\mu\text{m})^{1.887} \tag{20}$$

Based on this knowledge the effects of autocatalysis on the resulting drug release kinetics can adequately be taken into account.

Only a few mathematical theories have been reported in the literature describing the mass transport mechanisms involved in the control of drug release from *lipid-based implants*. Recently, the following analytical solution of Fick's second law of diffusion has been proposed to quantify protein release from triglyceride-based cylinders (Guse et al., 2006):

$$\frac{M_t}{M_\infty} = 1 - \frac{32}{\pi^2}\sum_{n=1}^{\infty}\frac{1}{q_n^2}\exp\left(-\frac{q_n^2}{{R_c}^2}Dt\right) \times \sum_{p=0}^{\infty}\frac{1}{(2p+1)^2}\exp\left(-\frac{(2p+1)^2\pi^2}{H^2}Dt\right) \tag{21}$$

where M_t and M_∞, represent the absolute cumulative amounts of protein released at time t and infinite time, respectively; the q_ns are the roots of the Bessel function of the first kind of zero order ($J_0(q_n) = 0$), and R_c and H denote the radius and height of the cylinder.

In several cases, good agreement between theory and experiment was obtained (e.g., with lysozyme-loaded, glycerol tripalmitate-based cylinders), indicating that drug release is primarily diffusion-controlled. However, the preparation method of the implant (e.g., direct compression versus compression of a powder obtained by lyophilization of a drug- and lipid-containing emulsion) and composition of the system (e.g., presence of water-soluble excipients) can significantly alter the underlying drug release mechanisms and release kinetics. So far there is only sparse knowledge available on the relationships between the different formulation and processing parameters and the consequent mass transport processes.

3. Drug transport within the living brain tissue

3.1. Overall mass transport mechanisms

The physical and chemical phenomena which can affect the transport of a drug within the living brain tissue are very complex and yet not fully understood. An excellent overview on the importance of diffusion and related processes has been given by Nicholson (Tao and Nicholson, 1996; Nicholson, 2001). He and his co-workers as well as the group of Saltzman made major contributions towards a better understanding of these phenomena (Reinhard et al., 1991; Saltzman and Radomsky, 1991; Dang et al., 1994; Haller and Saltzman, 1998a, 1998b; Fung et al., 1998).

A large variety of processes can be involved in the transport of the drug once it is released from the dosage form to its target site(s), including:

- diffusion within the extracellular space (ECS)
- reversible and irreversible binding to the extracellular matrix (which is built of long-chain macromolecules)
- degradation (e.g. by enzymes or hydrolysis)
- passive or active uptake into CNS cells (by diffusion or receptor-mediated internalization)
- release from endolysosomes into the cytosol
- diffusion and convection within the cytosol of the cells
- uptake into the cell nuclei (where appropriate)
- elimination into the blood stream
- bulk flow within the extracellular space
- direction dependent drug transport (anisotropy), because the brain is not one homogeneous mass

Fig. 7 shows a schematic representation of some of these processes.

So far, most models focus on the drug transport within the extracellular space, which represents only about 20% of the total brain volume in healthy humans. The geometry of this extracellular space is similar to that of the water phase of an aqueous foam. Drug transport in it can often surprisingly well be described on the basis of Fick's second law of diffusion. Important aspects to be taken into account include the volume fraction in which diffusion can take place and the tortuosity of the diffusion pathways. Recently, Nicholson and colleagues studied the effects of the geometry of CNS cells on the tortuosity of the extracellular space (Tao and Nicholson, 2004; Hrabetova and Nicholson, 2004; Tao et al., 2005). Considering uniformly spaced convex cells, they found that the presence of dead-space microdomains can help to explain the difference between the experimentally measured tortuosity and theoretically calculated values. Swanson et al. (2002) have studied the heterogeneous growth of tumours and the rarely uniform delivery of drugs to tumours as further complicating factors in predicting and measuring outcomes.

It has to be pointed out that many brain diseases can significantly affect the environment for drug transport within the brain (Sykova, 1997, 2004). For example, cellular swelling can lead to a significant shrinkage of the extracellular space, because the total brain volume is restricted by the rigid cranium. Tortuosity can be altered significantly: in some cases, the non-physiological mass transport conditions are not the consequence of the disease, but its cause: The adequate transport of oxygen, glucose, neurotransmitters and many other substances is vital for a normal functioning of the brain and when disrupted can cause significant pathologies. In addition, the conditions for drug transport within the brain can be significantly age-dependent. Lehmenkuhler et al. (1993) showed that the volume fraction of the extracellular space of rats decreases from about 0.36–0.46 in 2–3-day-old animals to 0.20–0.23 in 21-day-old animals. Obviously, these changes can strongly affect the transport of intracranially administered drugs.

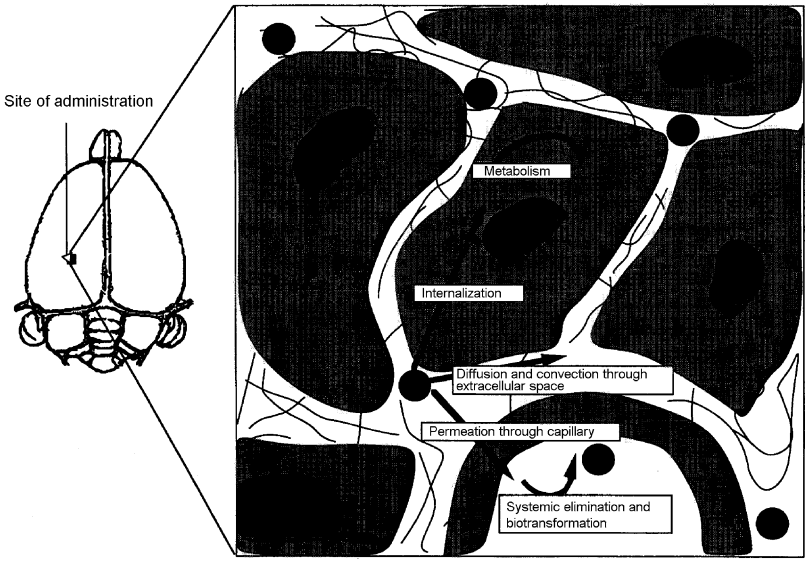

Fig. 7. Schematic presentation of some of the processes that can be involved in drug transport through the living brain tissue (indicated in the figure). The black circles represent drug molecules in the interstitial space (reprinted with permission of Springer Science and Business Media from Fung et al., 1996). Convection-enhanced delivery of drugs is discussed by Yang et al. (2002).

3.2. Experimental measurement techniques

The measurement of drug transport within the brain is not straightforward and sometimes artifact creation can be a major obstacle to obtaining reliable results. The most frequently used techniques include: (i) autoradiography and fluorescence microscopy, (ii) microdialysis, (iii) ion-selective microelectrode measurements and (iv) magnetic resonance imaging (MRI).

Autoradiographical methods (also called radiotracer methods, which were the first techniques used to quantify mass transport in the brain in a quantitative way) involve: (i) administration of a radioactive or radio-labeled drug into the brain tissue of animals, (ii) sacrificing the animal at predetermined time intervals, (iii) fixing the radiotracer in the tissue, (iv) slicing the brain and (v) measuring the radioactivity per volume tissue. From these measurements, concentration distance profiles can be generated. An interesting example has been reported by Roullin et al. (2002). [^{3}H](6)-5-Fluorouracil encapsulated within PLGA-based microparticles was administered to the brains of both healthy and C6 glioma-bearing rats. Fig. 8 shows radioactivity distribution in the two obtained 168 h after microparticle administration. The monitoring of drug transport using fluorescence microscopy is based on the same principle, except that the drug is not detected by radioactivity but by fluorescence measurements (Nicholson and Tao, 1993; Nicholson, 2001). The drug is either intrinsically fluorescent or has been fluorescently labeled. Advantages of both autoradiography and fluorescence microscopy include the possibility of measuring very low drug concentrations (<100 ng/ml) and the ability to map regional and/or direction-dependent mass transport within the brain. Disadvantages include the high number of animals needed and the time-consuming nature of the techniques.

Microdialysis is also a frequently used technique to measure drug transport in the CNS. The reviews of Boschi and Scherrmann (2000), Hammarlund-Udenaes (2000) and Peters et al. (2000) give a comprehensive overview on the current state of the art. The basic idea is to implant a small probe which is constructed with a hollow fiber dialysis membrane (being permeable for the drug of interest) into the living brain tissue. Fig. 9 shows a schematic illustration of such a probe, through which artificial cerebrospinal fluid is pumped at a well-controlled rate. Based on the drug concentrations measured in the fluid that enters and leaves the probe (c_{in} and c_{out}) and on the flow rate of the liquid, the drug concentration in the surrounding environment ($c_{environment}$) can be calculated. Several theoretical models have been proposed to evaluate the obtained experimental results (Stahle, 2000). If different probes are implanted simultaneously at several positions, a certain spatial resolution can be provided. However, the number of probes that are implanted at the same time is limited and care has to be taken because the presence of the probes in the living tissue can cause inflammation and, thus, artificial/pathologic transport conditions. The use of microdialysis in oncological research is discussed by Alanazi et al. (2004) and Brunner and Müller (2002) and in the review by Chu and Gallo (2000). One advantage of this technique is that the concentration of the drug that is mobile in the extracellular space (being able to diffuse through the dialysis membrane) can be

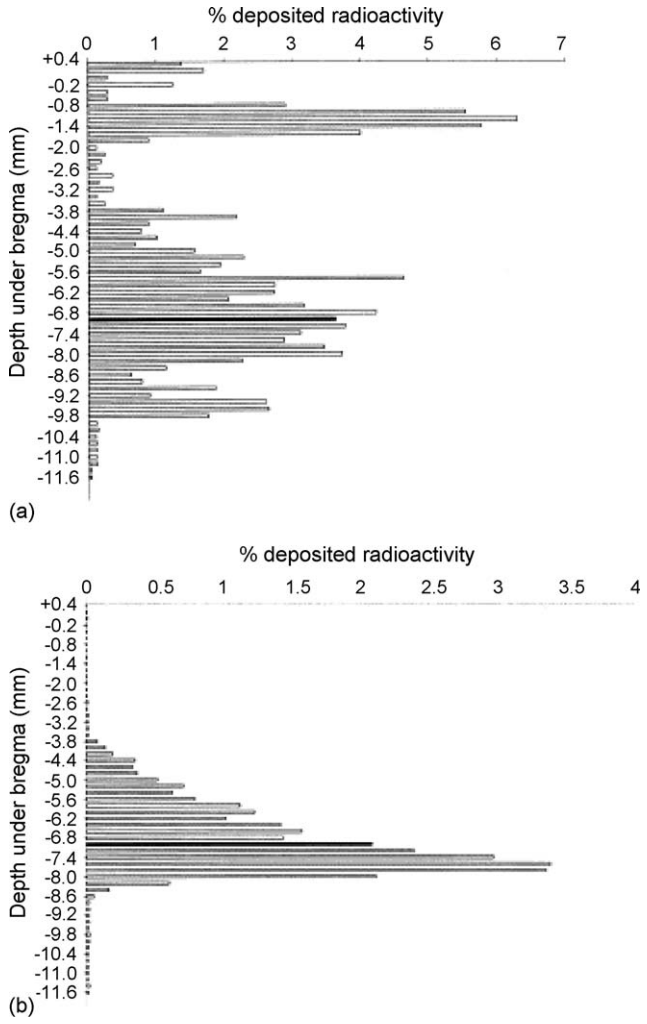

Fig. 8. Monitoring of the drug distribution within: (a) healthy and (b) tumor-bearing rat brain using autoradiography. Relative radioactivity measured as a function of the distance from the bregma; 168 h after intracranial administration of [^{3}H]5-FU-loaded microspheres. The black bars indicate the administration site (7 mm under the bregma) (reprinted with permission from Roullin et al., 2002).

measured. Thus, in combination with other techniques detecting the total drug concentration (e.g., fluorescence microscopy), the ratio of mobile drug in the extracellular space to immobile drug (including bound drug in the extracellular space plus bound and unbound drug in the intracellular space and membranes) can be determined. Another major advantage of microdialysis is that the measurements can be performed in the conscious living mouse, as illustrated in Fig. 10. However, in practice success may well depend on the drug substance being studied, its intrinsic solubility in brain fluids, its binding to brain tissue and its molecular size. Paclitaxel recovery by microdialysis even in in vitro conditions was low. The molecular weight of paclitaxel is 853.9. It has an aqueous solubility of 0.01 mg/ml (10 μg/ml) and a diffusion coefficient of 9×10^{-6} cm^2/s (Fung et al., 1998), a log P value of 3.5, a $t_{1/2}$ (degradation) of 17,000 min. It binds to α1-acid glycoprotein, BSA and calf-serum. Diffusion is consequently reduced in the presence of these by 41, 49 and 74%, respectively (Lovich et al., 2001). Paclitaxel is slowly released

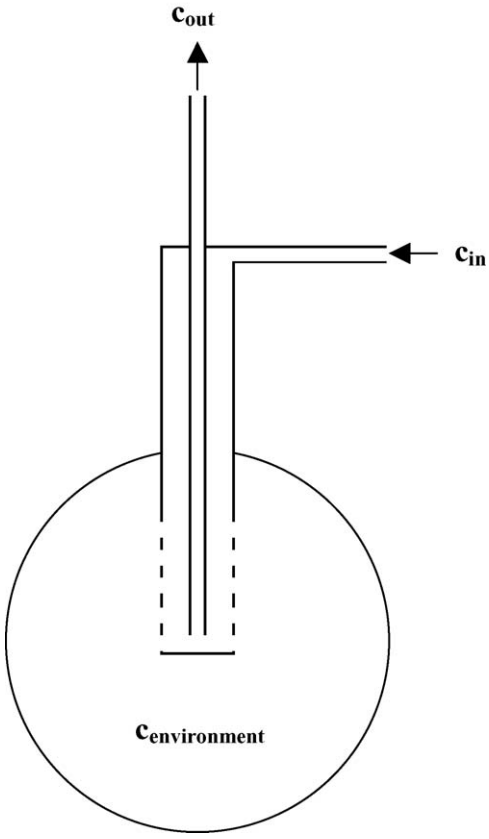

Fig. 9. Schematic presentation of a microdialysis probe used to monitor drug transport in living brain tissue; c_{in}/c_{out} and $c_{environment}$ denote respectively the drug concentration in the fluid that enters/leaves the dialysis probe and the concentration in the surrounding environment.

from intracellular binding sites and binds to intracellular and extracellular macromolecules, it increases microtubule formation and it experiences hindered mobility within microtubules (Ross and Fygenson, 2003). Models of transport in the brain have to account for all of these factors for this drug. In attempts to

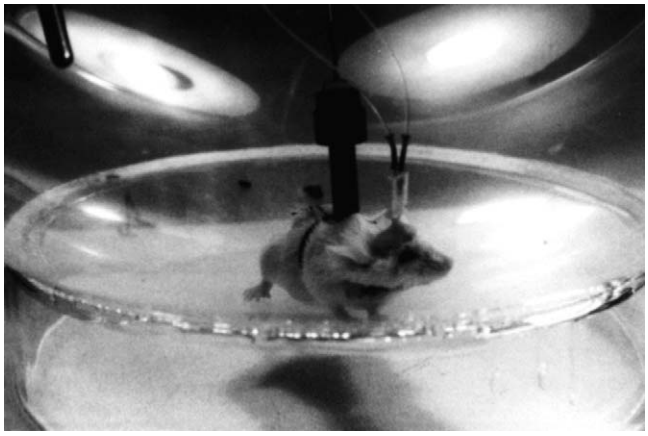

Fig. 10. Microdialysis in a conscious living mouse to monitor drug distribution within the brain. The microdialysis probe is implanted in the brain. At a well-controlled flow rate a fluid enters and leaves the probe through the two tubes. The wire with collar connector attached to the collar around the body of the animal turns a swivel allowing its free movement, and also supports the tubing (reprinted with permission from Boschi and Scherrmann, 2000).

increase the rate of paclitaxel released from simple suspensions of the drug, surfactant can be used. (Hussain et al., unpublished). However, Henningsson et al. (2001) have shown that this can lead to complications as nonionic surfactants such as Cremophor EL, decrease by solubilisation the free fraction of drug available for diffusion and uptake.

The insensitivity of so-called microdialysis aero-flux methods to non-linear uptake and release processes is the subject of a paper by Chen (2003). There is also evidence from work with brain slices that the insertion of probes might well compress tissue in the immediate surroundings to create a barrier to diffusion into the probe. It is surmised that the insertion of implants into brains may also distort tissue to create barriers to the release of the drug from the implanted material, and that this might lead, in itself, to asymmetric drug distribution (Fig. 11).

Ion-selective microelectrode measurements for the measurement of mass transport in the brain tissue have been pioneered by Nicholson and co-workers (Nicholson, 1985, 2001; Nicholson and Phillips, 1981; Nicholson and Sykova, 1998). The principle of this technique is to administer a marker ion (e.g., tetramethyl ammonium$^+$ cations, TMA$^+$) from a very small source (that can be approximated by a point, e.g., a micropipette), using either pressure injection or iontophoretic current. In the simplest case, the injection is very rapid (a finite pulse in time) and can be described by a δ-function. Then, the concentration of this ion is selectively measured with a special microelectrode at a known distance from the source (often 50–150 μm away) as a function of time. Major advantages of this method include a high time resolution (in the order of 1 min) and the possibility to measure drug transport in very small regions. A drawback is the restriction to ions which can be selectively measured by the microelectrode, hence the technique is not universally applicable.

Due to the significant advances in the field of magnetic resonance imaging (MRI), also this technique can be used to measure drug transport in vivo in the brain tissue, sometimes even in a non-invasive manner (Kroenke and Neil, 2004). For example, Ramaprasad and co-workers (Ramaprasad, 1994; Ramaprasad and Komoroski, 1994) monitored the diffusion of lithium within rat brain using stimulated echo acquisition mode spectroscopy (STEAM). The diffusivities of other substances, such as water, lactate, glucose, mannitol and polyethylenglycol have been measured in rat brain using MRI techniques by several laboratories (Duong et al., 1998, 2001; Pfeuffer et al., 2000; Silva et al., 2002).

3.3. Mathematical theories

Interestingly, only a very limited number of mathematical models have been reported in the literature that quantitatively describe drug transport in living brain tissue. In particular, Nicholson and co-workers and the group of Saltzman have made major contributions to this field. Jain's work has also led to a better appreciation of the complexities of diffusion in the brain (Jain, 2001; Mollica et al., 2003; Pluen et al., 2001; Ramanujan et al., 2002).

An excellent overview on the mathematical description of the most important phenomena involved in mass transport within

(a)

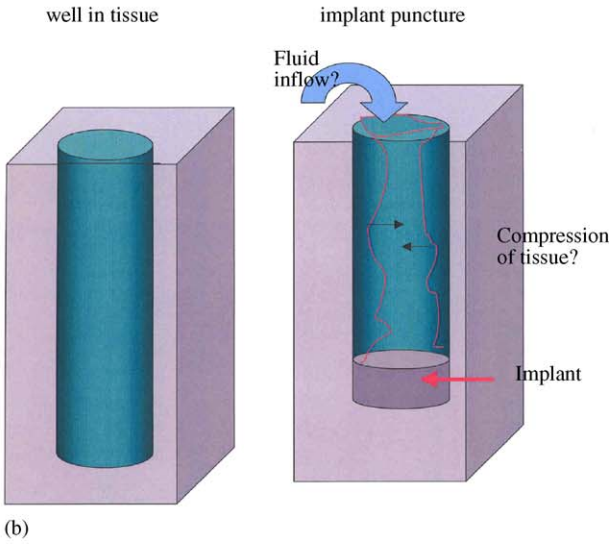

(b)

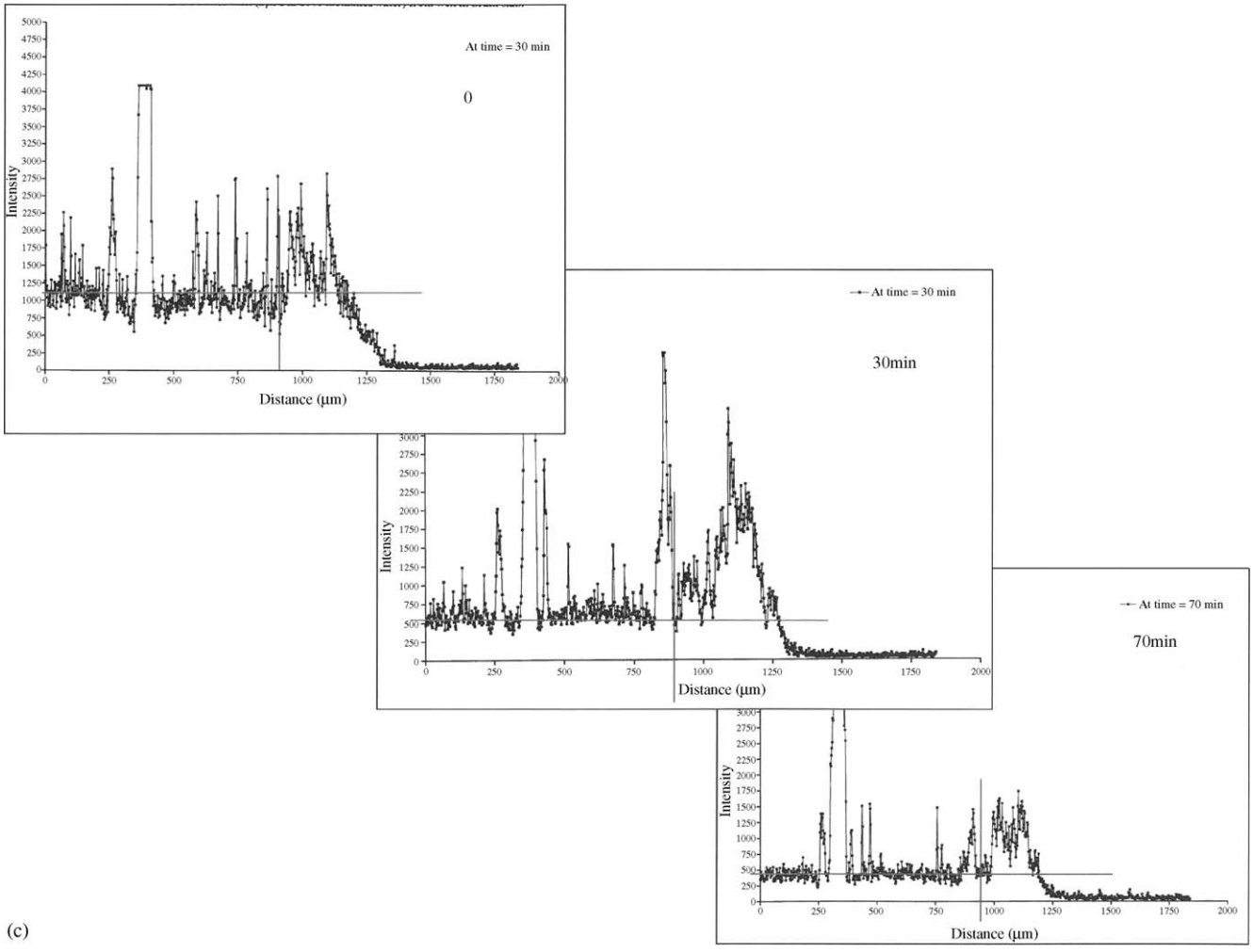

(c)

Fig. 11. (a) A schematic diagram of the potential for the change in the compression of tissue surrounding the channel used to insert an implant, providing an additional barrier to diffusion from the implant. This suggestion arose from studies of brain slices and confocal images of diffusion of fluorescent paclitaxel BODIPY (Florence et al., unpublished) results of which are shown in (b) and (c). (b) Reproduces confocal microscopy images of the edge of the well used to insert drug solution and (c) a fluorescence intensity trace, which also suggests that drug is binding to tissue fragments in the well (hence the fluorescence "spikes").

the living brain tissue has been given by Nicholson (2001). This includes the theoretical background required for the evaluation of experimental results obtained with different types of in vivo drug transport measurements. For example, if ion-selective microelectrodes are used to monitor mass transport within the brain, the following equation can be applied to quantify the ion concentration, c, at the distance r from the injection site as a function of time t:

$$c = \frac{Uc_f}{\alpha}\frac{\lambda^3}{(4Dt\pi)^{3/2}}\exp\left(-\frac{\lambda^2 r^2}{4Dt} - k't\right) \tag{22}$$

Here, U and c_f denote the volume and concentration of the injected ion solution (the injection is very rapid and the volume very small so that the source density can be described by a product of δ-functions in both space and time); α and λ denote the volume fraction and tortuosity of the extracellular space in which diffusion occurs; D represents the diffusion coefficient of the ion; and k' is a first order rate constant (e.g., describing linear uptake into CNS cells).

If the injection volume U cannot be assumed to be confined to a point upon administration (if the source density cannot be described by a product of δ-functions in space), but if it fills a finite volume of the brain tissue, then the concentration at the microelectrode at the distance r can be calculated as follows:

$$c = \frac{c_f}{2}\left[\mathrm{erf}\,(f_+) - \mathrm{erf}\,(f_-) + \frac{2}{\lambda r}\sqrt{\frac{Dt}{\pi}} \times \left[\exp(-f_+^2) - \exp(-f_-^2)\right]\right]\exp(-k't) \tag{23}$$

with

$$f_\pm = (r \pm b)\frac{\lambda}{2\sqrt{Dt}} \tag{24}$$

and

$$b = \frac{U}{\alpha} \tag{25}$$

Using these equations and sets of experimental results, the diffusion coefficient of the respective ion within the brain tissue can be determined.

To quantitatively describe drug transport within the living brain, Saltzman and Radomsky (1991) proposed an interesting mathematical model, considering drug diffusion from intracranially administered delivery systems as well as drug elimination. The theory is based on the following assumptions:

(i) At the surface of the dosage forms the concentration of the drug is constant.
(ii) The elimination of the drug follows first order kinetics (the elimination rate of the drug is proportional to its concentration).
(iii) Diffusion is isotropic (does not dependent on a spatial direction).[1]
(iv) Convectional processes are negligible.
(v) Drug release from the cylindrical devices occurs only in axial direction.

The model is based on Fick's second law of diffusion (considering one dimension), which is coupled with a first order elimination term:

$$\frac{\partial c}{\partial t} = D\left(\frac{\partial^2 c}{\partial x^2}\right) - kc \tag{26}$$

where c is the concentration of the drug within the brain tissue; t is time ($t = 0$ at the time of device administration); D represents the apparent diffusion coefficient of the drug within the brain; x is the spatial coordinate (distance from the interface "delivery system–brain tissue"); and k is the first order elimination rate constant of the drug.

The following initial and boundary conditions were considered:

$$c = 0 \quad \text{for } t = 0; \quad x \geq a \tag{27}$$

$$c = c_0 \quad \text{for } t > 0; \quad x = a \tag{28}$$

$$c = 0 \quad \text{for } t > 0; \quad x \to \infty \tag{29}$$

where a is the half-thickness of the cylindrical dosage form and c_0 the (constant) drug concentration at the surface of the device.

Eq. (27) indicates that the brain tissue is free of drug prior to the administration of the dosage form. Eq. (28) states that the constant drug concentration at the interface "dosage form–brain tissue" is time-independent, and Eq. (29) expresses the fact that the drug concentration vanishes to zero at large distances from the cylinder.

Assuming steady state conditions where the concentration of the drug within the brain tissue does not vary with time, only with position, this set of equations can be solved to give:

$$c = c_0 \exp\left(-a\sqrt{\frac{k}{D}}\left(\frac{x}{a} - 1\right)\right) \tag{30}$$

On the other hand, considering non-steady state conditions (in which the drug concentration varies with time and position), the following solution can be derived:

$$c = \frac{c_0}{2}\left[\exp\left(-x\sqrt{\frac{k}{D}}\right)\mathrm{erfc}\left(\frac{x}{\sqrt{4Dt}} - \sqrt{kt}\right) + \exp\left(x\sqrt{\frac{k}{D}}\right)\mathrm{erfc}\left(\frac{x}{\sqrt{4Dt}} + \sqrt{kt}\right)\right] \tag{31}$$

Both Eqs. (30) and (31) allow calculation of the drug concentration at any distance from the axial surface of the cylindrical

[1] Diffusion in the brain is frequently anisotropic: see Papadakis, Xing et al. (1999) and the calculation of an anisotropy index. This may be exacerbated by the process of implantation of delivery matrices as described in Fig. 11.

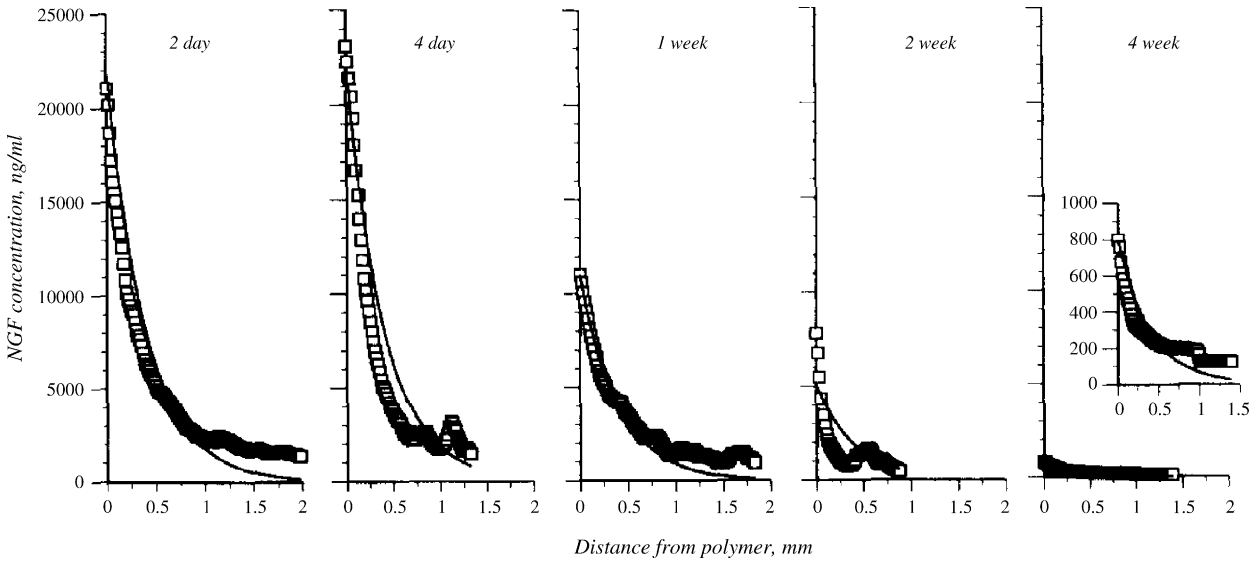

Fig. 12. Comparing experiment (symbols) and theory (curve): concentration profiles of radioactively labeled nerve growth factor within rat brain upon intracranial administration of a cylindrical controlled drug delivery system. The distance from the surface of the device is plotted on the *y*-axis; the times elapsed after implantation are indicated in the diagrams. The non steady state and steady state model of Krewson and Saltzman (Eqs. (31) and (30)) were fitted to the experimental results obtained at days 2 and 4 and 1, 2 and 4 weeks, respectively (reprinted with permission from Krewson and Saltzman, 1996).

dosage form. Fig. 12 shows examples of fittings of these models to sets of experimentally measured concentration profiles of radioactively labeled nerve growth factor (NGF). The drug was incorporated within cylindrical poly(ethylene-co-vinyl acetate) (EVAc)-based discs and intracranially administered to rats. After pre-determined time intervals (indicated in the figures), the animals were sacrificed, the brains sliced and the radioactivity measured. The non-steady state model (Eq. (31)) was fitted to the experimentally determined NGF concentration profiles at days 2 and 4, the steady state model (Eq. (30)) was fitted to the concentration profiles measured after 1, 2 and 4 weeks. Clearly, good agreement between theory and experiment was obtained in all cases. Thus, NGF transport through the living brain tissue seems to be dominated by diffusion and elimination. The partially observed deviations between theory and experiment might be attributable to experimental errors or violation of model assumptions (e.g., time-dependent drug concentrations at the surface of the delivery systems). Importantly, the distance that NGF can penetrate into the brain tissue is rather limited: after 2–3 mm its concentration decreases to only 10% of the maximal value (at the interface "dosage form–brain tissue"). Furthermore, Saltzman et al. (1999) compared the transport of NGF in rat brain upon its release from three different types of intracranial, controlled drug delivery systems: (i) slowly releasing EVAc discs, (ii) fast releasing PLGA-based microparticles and (iii) PLGA-based microparticles with an intermediate release rate. In all cases, good agreement between theory and experiment was obtained. An apparent diffusion coefficient of about 8×10^{-7} cm^2/s was determined for NGF in the rat brain.

Another model proposed by Saltzman and colleagues considers drug release from *spherical* dosage forms, drug diffusion, elimination *and convection* within the brain (Fung et al., 1996). The theory assumes that the brain is drug-free prior to device administration, that the drug concentration at the interface "dosage form–brain tissue" is constant and that the drug concentration far away from the administration site is negligible. Under these conditions, the following equation can be derived:

$$\frac{c}{c_0} = \frac{a}{2r}\left\{\operatorname{erfc}\left(\frac{r-a-vt}{2\sqrt{Dt}}\right) + \exp\left(\frac{(r-a)v}{D}\right)\operatorname{erfc}\left(\frac{r-a+vt}{2\sqrt{Dt}}\right)\right\}\exp(-kt) \quad (32)$$

Here, c is the concentration of the drug, being a function of time t and the radial distance from the center of the dosage form r; c_0 denotes the drug concentration at the interface "dosage form–brain tissue"; a is the radius of the spherical device; v is the apparent radial velocity in the extracellular space; and D denotes the apparent diffusivity of the drug in the brain.

Fitting this mathematical model to experimentally determined concentration profiles of BCNU (1,3-bis(2-chloroethyl)-1-nitrosourea; carmustine) in rat brain on intracranial administration of polyanhydride-based implants, good agreement between theory and experiment was obtained (Fung et al., 1996). Importantly, the interstitial fluid velocity could be estimated to equal 3.4 ± 1.7 mm/day based on these calculations.

Computer simulation of the delivery of etanidazole to brain tissues from PLGA wafers (Tan et al., 2003) compared delivery from a zero-order release system and a "double burst" wafer. The minimum threshold concentration of the drug is 5×10^{-7} mol/cm^3, only a factor of 10 lower than levels at which toxic effects appear (5×10^{-6} mol/cm^3). The zero-order system gives higher penetration over 75 days.

Levels of a cholesterol-based anticancer drug[2] administered in liposomes by intracerebral injection in a tumor (9L glioma)

[2] Cholesteryl 1,12-dicarba-closo-dodecaborane 1-carboxylate.

bearing rat model produced concentrations of drug in tumor tissue of 27.70 ± 5.54 μg/g at 2 h against 5.46 μg/g in the interstitium whereas at 6, 8 and 14 h the levels in tumor and normal tissues were identical (Alanazi et al., 2004).

3.3.1. Cell uptake

The concentration of drug in the extracellular space (ECS) and the apparent diffusivity of drug in the brain are important parameters. The concentration in the ECS is important in determining the spread of drug from the site of implantation, but does not indicate the concentration of drug within tumor cells, although there is a correlation between the two. Diffusion of drugs within the cytoplasm of individual cells will be many orders of magnitude lower than their diffusion in either water or the ECS. The diffusion coefficient of paclitaxel in water is, as stated above, 9×10^{-6} cm^2/s while the apparent diffusion coefficient of NGF (see above) is 8×10^{-7} cm^2/s in the ECS. In the cytoplasm organelles actin fibrils and other elements of the cytoskeleton as well as the molecular crowding in the cell interior serve to reduce diffusion, especially of proteins by several orders of magnitude. Collagen and hyaluronic acid gels have been used to mimic the content of these molecules in human and murine tumors (Ramanujan et al., 2002). Collagen can account for most of the diffusional hindrance in tumors. The variability of permeability coefficients in different tumors (over 10-fold, according to the data of Ramanujan et al. (2002)), and differences in the transport of molecules and particles in individual cells must be understood more extensively – and determined – before mathematical models will be able to predict outcome data. Complicating factors for some drugs include cell membrane *p*-glycoprotein pumps (e.g., paclitaxel induces *p*-gp) and cytoplasm character. Penetration of drugs into tumor spheroids – a useful model of avascular tumors – confirms the data in the brain by demonstrating with drugs such as doxorubicin and paclitaxel (Nicholson et al., 1997) penetration of a low order. Paclitaxel was unable to penetrate many layers of DLD-1 human colon adenocarcinoma spheroids. Boucher et al. (2001) report on "slow diffusing" and "fast-diffusing" groups of tumors, characterized by high and low collagen type I levels. The higher diffusivity in the ECS has advantages for drug spread but has a down side in that tumor cells can migrate through the ECS (Vargová et al., 2003). A positive correlation between increasing values of ECS volume fraction and proliferative activity in each tumor type was found. Tumour growth during the period of study obviously is a factor that ideally should be considered in modelling (Kansal et al., 2000).

Other complications arise because, for example, paclitaxel can induce apoptosis in epithelial cells in solid tumors, allowing greater drug penetration by reducing cell density (Ku et al., 1999; Jang et al., 2001).

4. Conclusions and future perspectives

Despite the considerable practical benefits of local controlled drug delivery to the brain, the mass transport mechanisms which determine drug transport within the dosage forms and through the living brain tissue are not yet fully understood. This can be attributed to the complexity of the involved phenomena. Several mathematical theories, comprehensive as well as simplified approaches have been applied, considering different types of physical and chemical processes determining the transport of the drug within the delivery systems or in the living brain tissue to the target site(s). Interestingly, there is a significant lack of mechanistically realistic models that adequately take into account both aspects: drug transport in the dosage forms and in the brain tissue. Ideally, such models would allow prediction of the effects of different formulation and processing parameters of different pharmaceutical devices (varying in both composition and size) on the resulting drug concentration–time profiles at the site(s) of action. These theories could be used to significantly facilitate the development and optimization of intracranially administered controlled drug delivery systems for the treatment of brain diseases. In particular, the number of in vivo studies required could be significantly reduced. In addition, the safety of these advanced treatment methods could be increased and their therapeutic effects optimized.

Acknowledgements

The authors are grateful for the support of this work by the European Commission (Research and Technological Development Project; BCDDS: Biodegradable Controlled Drug Delivery Systems for the Treatment of Brain Diseases; Contract No. QLK3-CT-2001-02226) and the French Association for Cancer Research "ARC" ("Association pour la Recherche sur le Cancer": postdoctoral fellowship for Florence Siepmann).

References

Abott, N.J., Romero, I.A., 1996. Transporting therapeutics across the blood-brain barrier. Mol. Med. Today 2, 106–113.

Alanazi, F., Halpern, D.S., Lu, D.R., 2004. Intracerebral diffusion of new cholesterol based anticancer conjugates in tumor bearing mice. J. Appl. Res. 4, 127–134.

Aubert-Pouessel, A., Venier-Julienne, M.C., Clavreul, A., Sergent, M., Jollivet, C., Montero-Menei, C.N., Garcion, E., Bibby, D.C., Menei, P., Benoit, J.P., 2004. In vitro study of GDNF release from biodegradable PLGA microspheres. J. Control. Release 95, 463–475.

Baker, R.W., 1987. Controlled Release of Biologically Active Agents. John Wiley & Sons, New York.

Baker, R.W., Lonsdale, H.K., 1974. Controlled release: mechanisms and rates. In: Tanquary, A.C., Lacey, R.E. (Eds.), Controlled Release of Biologically Active Agents. Plenum Press, New York, pp. 15–72.

Benoit, J.P., Faisant, N., Venier-Julienne, M.C., Menei, P., 2000. Development of microspheres for neurological disorders: From basics to clinical applications. J. Control. Release 65, 285–296.

Berkland, C., Kim, K., Pack, D.W., 2001. Fabrication of PLG microspheres with precisely controlled and monodisperse size distributions. J. Control. Release 73, 59–74.

Berkland, C., Kim, K., Pack, D.W., 2003. PLG microsphere size controls drug release rate through several competing factors. Pharm. Res. 20, 1055–1062.

Bittner, B., Maeder, K., Kroll, C., Borchert, H.H., Kissel, T., 1999. Tetracycline-HCl-loaded poly(DL-lactide-co-glycolide) microspheres prepared by a spray drying technique: influence of gamma-irradiation on radical formation and polymer degradation. J. Control. Release 59, 23–32.

Boschi, G., Scherrmann, J.M., 2000. Microdialysis in mice for drug delivery research. Adv. Drug Deliv. Rev. 45, 271–281.

Boucher, Y., Pluen, A., Ramanujan, S., McKee, T.D., Jain, R.K., 2001. American Society of Mechanical Engineers, Bioengineering Division, BED, 50, 97–98.

Brem, H., Mahaley, M.S., Vick, N.A., Black, K.L., Schold, S.C., Burger, P.C., Friedman, A.H., Ciric, I.S., Eller, T.W., Cozzens, J.W., Kenealy, J.N., 1991. Interstitial chemotherapy with drug polymer implants for the treatment of recurrent gliomas. J. Neurosurg. 74, 441–446.

Brem, H., Walter, K., Langer, R., 1993. Polymers as controlled drug delivery devices for the treatment of malignant brain tumors. Eur. J. Pharm. Biopharm. 27, 2–7.

Brem, H., Piantadosi, S., Burger, P.C., Walker, M., Selker, R., Vick, N.A., Black, K., Sisti, M., Brem, S., Mohr, G., Muller, P., Morawetz, R., Schold, S.C., The Polymer-brain Tumor Treatment Group, 1995a. Placebo-controlled trial of safety and efficacy of intraoperative controlled delivery by biodegradable polymers of chemotherapy for recurrent gliomas. Lancet 345, 1008–1012.

Brem, H., Ewend, M.G., Piantadosi, S., Greenhoot, J., Burger, P.C., Sisti, M., 1995b. The safety of interstitial chemotherapy with BCNU-loaded polymer followed by radiation therapy in the treatment of newly diagnosed malignant gliomas: phase I trial. J. Neurooncol. 26, 111–123.

Brem, H., Langer, R., 1996. Polymer-based drug delivery to the brain. Sci. Med., 52–61.

Brunner, A., Maeder, K., Goepferich, A., 1999. pH and osmotic pressure inside biodegradable microspheres during erosion. Pharm. Res. 16, 847–853.

Brunner, M., Müller, M., 2002. Microdialysis: an in vivo approach for measuring drug delivery in oncology. Eur. J. Clin. Pharmacol. 58, 227–234.

Charlier, A., Leclerc, B., Couarraze, G., 2000. Release of mifepristone from biodegradable matrices: experimental and theoretical evaluations. Int. J. Pharm. 200, 115–120.

Chasin, M., Langer, R., 1990. Biodegradable Polymers as Drug Delivery Systems. Marcel Dekker, New York.

Chen, K.C., 2003. Insensitivity of the microdialysis zero-flux method to nonlinear uptake and release processes. Neurosci. Res. 46, 251–256.

Chu, J., Gallo, J.M., 2000. Application of microdialysis to characterize drug disposition in tumors. Adv. Drug Deliv. Rev. 45, 243–253.

Cordes, E.H., Bull, H.G., 1974. Mechanism and catalysis for hydrolysis of acetals, ketals, and ortho esters. Chem. Rev. 94, 581–603.

Crank, J., 1975. The Mathematics of Diffusion. Clarendon Press, Oxford.

Dang, W., Colvin, O.M., Brem, H., Saltzman, W.M., 1994. Covalent coupling of methotrexate to dextran enhances the penetration of cytotoxicity into a tissue-like matrix. Cancer Res. 54, 1729–1735.

Duong, T.Q., Ackerman, J.J.H., Ying, H.S., Neil, J.J., 1998. Evaluation of extra- and intracellular apparent diffusion in normal and globall ischemic rat brain via 19F NMR. Magn. Reson. Med. 40, 1–13.

Duong, T.Q., Sehy, V.J., Yablonskiy, D.A., Snider, B.J., Ackerman, J.J.H., Neil, J.J., 2001. Extracellular apparent diffusion in rat brain. Magn. Reson. Med. 45, 801–810.

Ewend, M.G., Williams, J.A., Tabassi, K., Tyler, B.M., Babel, K.M., Anderson, R.C., Pinn, M.L., Brat, D.J., Brem, H., 1996. Local delivery of chemotherapy and concurrent external beam radiotherapy prolongs survival in metastatic brain tumor models. Cancer Res. 56, 5217–5223.

Faisant, N., Akiki, J., Siepmann, F., Benoit, J.P., Siepmann, J., 2006. Effects of the type of release medium on drug release from PLGA-based microparticles: experiment and theory. Int. J. Pharm. 314, 189–197.

Fung, L.K., Shin, M., Tyler, B., Brem, H., Saltzman, W.M., 1996. Chemotherapeutic drugs released from polymers: distribution of 1,3-bis(2-chloroethyl)-1-nitrosourea in the rat brain. Pharm. Res. 13, 671–682.

Fung, L.K., Ewend, M.G., Sills, A., Sipos, E.P., Thompson, R., Watts, M., Colvin, O.M., Brem, H., Saltzman, W.M., 1998. Pharmacokinetics of interstitial delivery of carmustine, 4-hydroperoxycyclophosphamide, and paclitaxel from a biodegradable polymer implant in the monkey brain. Cancer Res. 58, 672–684.

Goepferich, A., 1996a. Mechanisms of polymer degradation and erosion. Biomaterials 17, 103–114.

Goepferich, A., 1996b. Polymer degradation and erosion: mechanisms and applications. Eur. J. Pharm. Biopharm. 42, 1–11.

Goepferich, A., 1997a. Erosion of composite polymer matrices. Biomaterials 18, 397–403.

Goepferich, A., 1997b. Bioerodible implants with programmable drug release. J. Control. Release 44, 271–281.

Goepferich, A., 1997c. Mechanisms of polymer degradation and elimination. In: Domb, A., Kost, J., Wiseman, D. (Eds.), Handbook of Biodegradable Polymers. Harwood Academic Publishers, Amsterdam.

Goepferich, A., 1997d. Polymer bulk erosion. Macromolecules 30, 2598–2604.

Goepferich, A., Langer, R., 1993. Modeling of polymer erosion. Macromolecules 26, 4105–4112.

Goepferich, A., Langer, R., 1995a. Modeling monomer release from bioerodible polymers. J. Control. Release 33, 55–69.

Goepferich, A., Langer, R., 1995b. Modeling of polymer erosion in three dimensions – rotationally symmetric devices. AIChE J. 41, 2292–2299.

Goepferich, A., Shieh, L., Langer, R., 1995. Aspects of polymer erosion. Mater. Res. Soc. Symp. Proc. 394, 155–160.

Gref, R., Quellec, P., Sanchez, A., Calvo, P., Dellacherie, E., Alonso, M.J., 2001. Development and characterization of CyA-loaded poly(lactic acid)-poly(ethylene glycol)PEG micro- and nanoparticles. Comparison with conventional PLA particulate carriers. Eur. J. Pharm. Biopharm. 51, 111–118.

Grieg, N.H., 1987. Optimizing drug delivery to brain tumors. Cancer Treat. Rev. 14, 1–28.

Grossman, S.A., Reinhard, C., Colvin, O.M., Chasin, M., Brundrett, R., Tamargo, R.J., Brem, H., 1992. The intracerebral distribution of BCNU delivered by surgically implanted biodegradable polymers. J. Neurosurg. 76, 640–647.

Guse, C., Koennings, S., Kreye, F., Siepmann, F., Goepferich, A., Siepmann, J., 2006. Protein release from lipid-based implants: Elucidation of the underlying mass transport mechanisms. Int. J. Pharm. 314, 137–144.

Haller, M.F., Saltzman, W.M., 1998a. Localized delivery of proteins in the brain: can transport be customized? Pharm. Res. 15, 377–385.

Haller, M.F., Saltzman, W.M., 1998b. Nerve growth factor delivery systems. J. Control. Release 53, 1–6.

Hammarlund-Udenaes, M., 2000. The use of microdialysis in CNS drug delivery studies. Pharmacokinetic perspectives and results with analgesics and antiepileptics. Adv. Drug. Deliv. Rev. 45, 283–294.

Hedberg, E.L., Shih, C.K., Solchaga, L.A., Caplan, A.I., Mikos, A.G., 2004. Controlled release of hyaluronan oligomers from biodegradable polymeric microparticle carriers. J. Control. Release 100, 257–266.

Henningsson, A., Karlsson, M.D., Vigano, L., Gianni, L., Verweij, J., Sparreboom, A., 2001. Mechansim-based pharmacokinetic model for paclitaxel. J. Clin. Oncol. 19, 4065–4073.

Higuchi, T., 1961. Rate of release of medicaments from ointment bases containing drugs in suspensions. J. Pharm. Sci. 50, 874–875.

Hopfenberg, H.B., 1976. Controlled release from erodible slabs, cylinders, and spheres. In: Paul, D.R., Harris, F.W. (eds.), Controlled Release Polymeric Formulations, ACS Symp. Ser. No. 33. American Chemical Society, Washington, pp. 26–32.

Hrabetova, S., Nicholson, C., 2004. Contribution of dead-space microdomains to tortuosity of brain extracellular space. Neurochem. Int. 45, 467–477.

Jackson, J.K., Smith, J., Letchford, K., Babiuk, K.A., Machan, L., Signore, P., Hunter, W.L., Wang, K., Burt, H.M., 2004. Characterization of perivascular poly(lactic-co-glycolic acid) films containing paclitaxel. Int. J. Pharm. 283, 97–109.

Jain, R.K., 2001. Delivery of macromolecules and cellular medicine to solid tumors. Adv. Drug Deliv. Rev. 46, 49–68.

Jang, S.H., et al., 2001. Enhanced paclitaxel delivery to solid tumors by apoptosis-inducing pretreatment: effect of treatment schedule. J. Pharm. Exp. Ther. 296, 1035–1042.

Joshi, A., Himmelstein, K.J., 1991. Dynamics of controlled release from bioerodible matrices. J. Control. Release 15, 95–104.

Kansal, A.R., Torquato, S., Hash, G.R., Chiocca, E.A., Deisboeck, T.S., 2000. Simulated brain tumor growth using a 3-dimensional cellular automaton. J. Theor. Biol. 203, 367–382.

Klose, D., Siepmann, F., Elkharraz, K., Krenzlin, S., Siepmann, J., 2006. How porosity and size affect the drug release mechanisms from PLGA-based microparticles. Int. J. Pharm. 314, 198–206.

Ku, H.-J., Jang, S.H., et al., 1999. Determinants of paclitaxel penetration and accumulation in human solid tumors. J. Pharm. Exp. Ther. 290, 871–880.

Kostanski, J.W., Thanoo, B.C., DeLuca, P.P., 2000. Preparation, characterization, and in vitro evaluation of 1- and 4-month controlled release orntide PLA and PLGA microspheres. Pharm. Dev. Technol. 5, 585–596.

Kranz, H., Ubrich, N., Maincent, P., Bodmeier, R., 2000. Physicomechanical properties of biodegradable poly(D,L-lactide) and poly(D,L-lactide-co-glycolide) films in the dry and wet states. J. Pharm. Sci. 89, 1558–1566.

Krewson, C.E., Saltzman, W.M., 1996. Transport and elimination of recombinant human NGF during long-term delivery to the brain. Brain. Res. 727, 169–181.

Kroenke, C.D., Neil, J.J., 2004. Use of magnetic resonance to measure molecular diffusion within the brain extracellular space. Neurochem. Int. 45, 561–568.

Langer, R., 1980. Polymeric delivery systems for controlled drug release. Chem. Eng. Commun. 6, 1–48.

Langer, R., 1991. Polymer implants for drug delivery in the brain. J. Control. Release 16, 53–60.

Langer, R., Folkman, J., 1976. Polymers for the sustained release of proteins and other macromolecules. Nature 263, 797–800.

Langer, R.S., Wise, D.L., 1984. Medical Applications of Controlled Release. CRC Press, Boca Raton, FL.

Lee, J.S., An, T.K., Chae, G.S., 2005. Evaluation of in vitro and in vivo antitumor activity of BCNU-loaded PLGA wafers against 9L gliosarcoma. Eur. J. Pharm. Biopharm. 59, 169–175.

Lehmenkuhler, A., Sykova, E., Svoboda, J., Zilles, K., Nicholson, C., 1993. Extracellular space parameters in the rat neocortex and subcortical white matter during postnatal development determined by diffusion analysis. Neuroscience 55, 339–351.

Leo, E., Pecquet, S., Rojas, J., Couvreur, P., Fattal, E., 1998. Changing the pH of the external aqueous phase may modulate protein entrapment and delivery from poly(lactide-co-glycolide) microspheres prepared by a w/o/w solvent evaporation method. J. Microencapsul. 15, 421–430.

Leong, K.W., Brott, B.C., Langer, R., 1985. Bioerodible polyanhydrides as drug–carrier matrices. I: Characterization, degradation, and release characteristics. J. Biomed. Mater. Res. 19, 941–955.

Li, L., Schwendeman, S.P., 2005. Mapping neutral microclimate pH in PLGA microspheres. J. Control. Release 101, 163–173.

Lovich, M.A., et al., 2001. Carrier proteins determine local pharmacokinetics and alterial distribution of paclitaxel. J. Pharm. Sci. 90, 1324–1335.

Lurie, D.J., Maeder, K., 2005. Monitoring drug delivery processes by EPR and related techniques—principles and applications. Adv. Drug Deliv. Rev. 57, 1171–1190.

Maeder, K., 2005. Non-invasive spectroscopic and imaging techniques in drug delivery. Adv. Drug Deliv. Rev. 57, 1083–1084.

Maeder, K., Cremmilleux, Y., Domb, A.J., Dunn, J.F., Swartz, H.M., 1997. In vitro/in vivo comparison of drug release and polymer erosion from biodegradable P(FAD-SA) polyanhydrides: a noninvasive approach by the combined use of electron paramagnetic resonance spectroscopy and nuclear magnetic resonance imaging. Pharm. Res. 14, 820–826.

Menei, P., Benoit, J.P., Boisdron-Celle, M., Fournier, D., Mercier, P., Guy, G., 1994. Drug targeting into the central nervous system by stereotactic implantation of biodegradable microspheres. Neurosurgery 34, 1058–1064.

Menei, P., Venier, M.C., Gamelin, E., Saint-Andre, J.P., Hayek, G., Jadaud, E., Fournier, D., Mercier, P., Guy, G., Benoit, J.P., 1999. Local and sustained delivery of 5-fluorouracil from biodegradable microspheres for the radiosensitization of glioblastoma: a pilot study. Cancer 86, 325–330.

Menei, P., Jadaud, E., Faisant, N., Boisdron-Celle, M., Michalak, S., Fournier, D., Delhaye, M., Benoit, J.P., 2004. Stereotaxic implantation of 5-fluorouracil-releasing microspheres in malignant glioma. Cancer 100, 405–410.

Menei, P., Capelle, L., Guyotat, J., Fuentes, S., Assaker, R., Bataille, B., Francois, P., Dorwling-Carter, D., Paquis, P., Bauchet, L., Parker, F., Sabatier, J., Faisant, N., Benoit, J.P., 2005. Local and sustained delivery of 5-Fluorouracil from biodegradable microspheres for the radiosensitization of malignant glioma: a randomized phase II trial. Neurosurgery 56, 242–248.

Mittal, S., Cohen, A., Maysinger, D., 1994. In vitro effects of brain derived neurotrophic factor released from microspheres. NeuroReport 5, 2577–2582.

Mollica, F., Jain, R.K., Netta, P.A., 2003. A model for temporal heterogeneities of tumor blood flow. Microvasc. Res. 65, 56–60.

Moses, M.A., Brem, H., Langer, R., 2003. Advancing the field of drug delivery Taking aim at cancer. Cancer Cell 4, 337–341.

Nicholson, C., 1985. Diffusion from an injected volume of a substance in brain tissue with arbitrary volume fraction and tortuosity. Brain Res. 333, 325–329.

Nicholson, C., 2001. Diffusion and related transport mechanisms in brain tissue. Rep. Prog. Phys. 64, 815–884.

Nicholson, C., Phillips, J.M., 1981. Ion diffusion modified by tortuosity and volume fraction in the extracellular microenvironment of the rat cerebellum. J. Physiol. (Lond.) 321, 225–257.

Nicholson, C., Tao, L., 1993. Hindered diffusion of high molecular weight compounds in brain extracellular microenvironment measured with integrative optical imaging. Biophys. J. 65, 2277–2290.

Nicholson, C., Sykova, E., 1998. Extracellular space structure revealed by diffusion analysis. Trends Neurosci. 21, 207–215.

Nicholson, K.M., Dibby, M.C., Philips, R.M., 1997. Influence of drug exposure parameters on the action of paclitaxel in multicellular spheroids. Eur. J. Cancer 33, 1291–1298.

Papadakis, N.G., Xing, D., Houston, G.C., et al., 1999. A study of rotationally invariant and symmetric indeices of diffusion anisotropy. Magn. Reson. Imaging 17, 881–892.

Peppas, N.A., 1985. Analysis of Fickian and non-Fickian drug release from polymers. Pharm. Acta Helv. 60, 110–111.

Peppas, N.A., Korsmeyer, R.W., 1986. Dynamically swelling hydrogels in controlled release applications. In: Peppas, N.A. (Ed.), Hydrogels in Medicine and Pharmacy, vol. 3. CRC Press, Boca Raton, pp. 109–136.

Peters, J.L., Yang, H., Michael, A.C., 2000. Quantitative aspects of brain microdialysis. Anal. Chim. Acta 412, 1–12.

Pfeuffer, J., Tkac, I., Gruetter, R., 2000. Extracellular-intracellular distribution of glucose and lactate in the rat brain assessed non-invasively by diffusion-weighted ^{1}H nuclear magnetic resonance spectroscopy in vivo. J. Cerebral Blood Flow Metab. 20, 736–746.

Pluen, A., Boucher, Y., Ramanujan, S., McKee, T.D., Gohongi, T., di Tomaso, E., Brown, E.W.B., Izumi, Y., Campbell, R.B., Berk, D.A., Jain, R.K., 2001. Role of tumor-host interactions in interstitial diffusion of macromolecules: cranial vs. subcutaneous tumors. Proc. Natl. Acad. Sci. U.S.A. 98, 4628–4633.

Raman, C., Berkland, C., Kim, K.K., Pack, D.W., 2005. Modeling small-molecule release from PLG microspheres: effects of polymer degradation and nonuniform drug distribution. J. Control. Release 103, 149–158.

Ramanujan, S., Pluen, A., McKee, T.D., Brown, L.B., Boucher, Y., Jain, R.K., 2002. Diffusion and convection in collagen gels: implications for transport in tumor interstitium. Biophys. J. 83, 1650–1660.

Ramaprasad, S., 1994. In vivo ^{7}Li NMR diffusion studies in rat brain. Magn. Reson. Imaging 12, 523–529.

Ramaprasad, S., Komoroski, R.A., 1994. NMR imaging and localized spectroscopy of lithium. Lithium 5, 127–138.

Reinhard, C.S., Radomsky, M.L., Saltzman, W.M., Hilton, J., Brem, H., 1991. Polymeric controlled release of dexamethasone in normal rat brain. J. Control. Release 16, 331–339.

Richardson, J.C., Bowtell, R.W., Maeder, K., Melia, C.D., 2005. Pharmaceutical applications of magnetic resonance imaging (MRI). Adv. Drug Deliv. Rev. 57, 1191–1209.

Ritger, P.L., Peppas, N.A., 1987. A simple equation for description of solute release. I. Fickian and non-Fickian release from non-swellable devices in the form of slabs, spheres, cylinders or discs. J. Control. Release 5, 23–36.

Ross, J.L., Fygenson, D.K., 2003. Mobility of taxol in microtubule bundles. Biophys. J. 84, 3957–3959.

Ron, E., Langer, R., 1992. Erodible systems. In: Kydonieus, A. (Ed.), Treatise on Controlled Drug Delivery. Marcel Dekker, pp. 199–224.

Roullin, V.G., Deverre, J.R., Lemaire, L., Hindre, F., Venier-Julienne, M.C., Vienet, R., Benoit, J.P., 2002. Anti-cancer drug diffusion within living rat brain tissue: an experimental study using [^{3}H](6)-5-fluorouracil-loaded PLGA microspheres. Eur. J. Pharm. Biopharm. 53, 293–299.

Saltzman, W.M., Radomsky, M.L., 1991. Drugs released from polymers: diffusion and elimination in brain tissue. Chem. Eng. Sci. 46, 2429–2444.

Saltzman, W.M., Mak, M.W., Mahoney, M.J., Duenas, E.T., Cleland, J.L., 1999. Intracranial delivery of recombinant nerve growth factor: release kinetics and protein distribution for three delivery systems. Pharm. Res. 16, 232–240.

Siepmann, J., Goepferich, A., 2001. Mathematical modeling of bioerodible, polymeric drug delivery systems. Adv. Drug Deliv. Rev. 48, 229–247.

Siepmann, J., Peppas, N.A., 2001. Modeling of drug release from delivery systems based on hydroxypropyl methylcellulose (HPMC). Adv. Drug Deliv. Rev. 48, 139–157.

Siepmann, J., Faisant, N., Benoit, J.P., 2002. A new mathematical model quantifying drug release from bioerodible microparticles using Monte Carlo simulations. Pharm. Res. 19, 1885–1893.

Siepmann, J., Elkharraz, K., Siepmann, F., Klose, D., 2005. How autocatalysis accelerates drug release from PLGA-based microparticles: A quantitative treatment. Biomacromolecules 6, 2312–2319.

Silva, M.D., Omae, T., Helmer, K.G., Li, F., Fisher, M., Sotak, C.H., 2002. Separating changes in the intra- and extracellular water apparent diffusion coefficient following focal cerebral ischemia in the rat brain. Magn. Reson. Med. 48, 826–837.

Sipos, E.P., Tyler, B., Piantadosi, S., Burger, P.C., Brem, H., 1997. Optimizing interstitial delivery of BCNU from controlled release polymers for the treatment of brain tumors. Cancer Chemother. Pharmacol. 39, 383–389.

Stahle, L., 2000. On mathematical models of microdialysis: Geometry, steady-state models, recovery and probe radius. Adv. Drug Deliv. Rev. 45, 149–167.

Swanson, K.R., Alvord, E.C., Murray, J.D., 2002. Quantifying efficacy of chemotherapy of brain tumors with homogeneous and heterogeneous drug delivery. Acta Biother. 50, 223–237.

Sykova, E., 1997. The extracellular space in the CNS: Its regulation, volume and geometry in normal and pathological neuronal function. Neuroscientist 3, 28–41.

Sykova, E., 2004. Diffusion properties of the brain in health and disease. Neurochem. Int. 45, 453–466.

Tamargo, R.J., Sills, A.K.J., Reinhard, C.S., Pinn, M.L., Long, D.M., Brem, H., 1991. Interstitial delivery of dexamethasone in the brain for the reduction of peritumoral edema. J. Neurosurg. 74, 956–961.

Tamargo, R.J., Myseros, J.S., Epstein, J.I., Yang, M.B., Chasin, M., Brem, H., 1993. Interstitial chemotherapy of the 9L gliosarcoma: controlled release polymers for drug delivery in the brain. Cancer Res. 53, 329–333.

Tan, W.H.K., Wang, F., Lee, T., Wang, C.H., 2003. Computer simulation of the delivery of etanidazole to brain tumor from PLGA wafers: comparison between lesser and double burst release systems. Biotech. Bioeng. 82, 278–288.

Tao, L., Nicholson, C., 1996. Diffusion of albumins in rat cortical slices and relevance to volume transmission. Neuroscience 75, 839–847.

Tao, L., Nicholson, C., 2004. Maximum geometrical hindrance to diffusion in brain extracellular space surrounding uniformly spaced convex cells. J. Theor. Biol. 229, 59–68.

Tao, A., Tao, L., Nicholson, C., 2005. Cell cavities increase tortuosity in brain extracellular space. J. Theor. Biol. 234, 525–536.

Thombre, A.G., 1992. Theoretical aspects of polymer biodegradation: Mathematical modeling of drug release and acid-catalyzed poly(ortho-ester) biodegradation. In: Vert, M., Feijen, J., Albertsson, A., Scott, G., Chiellini, E. (Eds.), Biodegradable Polymers and Plastics. Redwood Press, Melksham, pp. 214–228.

Thombre, A.G., Himmelstein, K.J., 1985. A simultaneous transport-reaction model for controlled drug delivery from catalyzed bioerodible polymer matrices. AIChE J. 31, 759–766.

Valtonen, S., Timonen, U., Toivanen, P., Kalimo, H., Kivipelto, L., Heiskanen, O., Unsgaard, G., Kuurne, T., 1997. Interstitial chemotherapy with carmustine-loaded polymers for high-grade gliomas: a randomized double-blind study. Neurosurgery 41, 44–49.

Vargová, L., Homola, A., Zámečnik, J., Tichý, M., Beneš, V., Syková, E., 2003. Diffusion parameters of the extracellualr space in human gliomas. Glia 42, 77–88.

Vergnaud, J.M., 1993. Controlled Drug Release of Oral Dosage Forms. Ellis Horwood, Chichester.

von Burkersroda, F., Schedl, L., Goepferich, A., 2002. Why degradable polymers undergo surface erosion or bulk erosion. Biomaterials 23, 4221–4231.

Wang, P.P., Frazier, J., Brem, H., 2002a. Local drug delivery to the brain. Adv. Drug Deliv. Rev. 54, 987–1013.

Wang, J., Wang, B.M., Schwendeman, S.P., 2002b. Characterization of the initial burst release of a model peptide from poly(D,L-lactide-co-glycolide) microspheres. J. Control. Release 82, 289–307.

Woo, B.H., Kostanski, J.W., Gebrekidan, S., Dani, B.A., Thanoo, B.C., DeLuca, P.P., 2001. Preparation, characterization and in vivo evaluation of 120-day poly(D,L-lactide) leuprolide microspheres. J. Control. Release 75, 307–315.

Yang, M.B., Tamargo, R.J., Brem, H., 1989. Controlled delivery of 1,3-bis(2-chloroethyl)-1-nitrosourea from ethylene-vinyl acetate copolymer. Cancer Res. 49, 5103–5107.

Yang, W., Barth, R.F., Adams, D.M., et al., 2002. Convection-enhanced delivery. Cancer Res. 62, 6552–6558.

Yilmaz, G., Jongboom, R.O., Feil, H., van Dijk, C., Hennink, W.E., 2004. Permeation of volatile compounds through starch films. Biomacromolecules 5, 650–656.

Zygourakis, K., 1989. Discrete simulations and bioerodible controlled release systems. Polym. Prep. ACS 30, 456–457.

Zygourakis, K., 1990. Development and temporal evolution of erosion fronts in bioerodible controlled release devices. Chem. Eng. Sci. 45, 2359–2366.

Zygourakis, K., Markenscoff, P.A., 1996. Computer-aided design of bioerodible devices with optimal release characteristics: a cellular automata approach. Biomaterials 17, 125–135.